Copyright Warning & Restrictions

The copyright law of the United States (Title 17, United States Code) governs the making of photocopies or other reproductions of copyrighted material.

Under certain conditions specified in the law, libraries and archives are authorized to furnish a photocopy or other reproduction. One of these specified conditions is that the photocopy or reproduction is not to be "used for any purpose other than private study, scholarship, or research." If a, user makes a request for, or later uses, a photocopy or reproduction for purposes in excess of "fair use" that user may be liable for copyright infringement,

This institution reserves the right to refuse to accept a copying order if, in its judgment, fulfillment of the order would involve violation of copyright law.

Please Note: The author retains the copyright while the New Jersey Institute of Technology reserves the right to distribute this thesis or dissertation

Printing note: If you do not wish to print this page, then select "Pages from: first page # to: last page #" on the print dialog screen

HEAT TRANSFER COEFFICIENTS

OF

NON-NEWTONIAN SLURRIES

IN

LAMINAR FLOW

A THESIS

SUBMITTED TO THE FACULTY

OF

THE DEPARTMENT OF CHEMICAL ENGINEERING

OF

NEWARK COLLEGE OF ENGINEERING

by

ROBERT F. ROTH, B.S.Ch.E.

and

DAVID B. SWANSON, B.S.Ch.E.

IN PARTIAL FULFILLMENT OF THE REQUIREMENTS FOR THE DEGREE

OF MASTER OF SCIENCE IN CHEMICAL ENGINEERING.

NEWARK, NEW JERSEY

SEPTEMBER, 1961

APPROVAL OF THESIS

FOR

DEPARTMENT OF CHEMICAL ENGINEERING

NEWARK COLLEGE OF ENGINEERING

BY

FACULTY COMMITTEE

APPROVED: _____

_____

_____

NEWARK, NEW JERSEY

SEPTEMBER, 1961

TABLE OF CONTENTS

Subject	Page
Acknowledgements	iv
List of Figures	v
List of Tables	vi
Abstract	1
Introduction	2
Theory	3
Literature Search	8
Description of Apparatus	14
Experimental Procedure	19
Experimental Results	22
Discussion of Results	37
Conclusion	43
Nomenclature	45
References	47
Appendix - Sample Calculations	49

ACKNOWLEDGEMENT

The authors express their sincere appreciation to Dr. Jerome J. Salamone for his assistance, confidence, interest and guidance in carrying this project to a successful conclusion.

The authors gratefully acknowledge the efforts of Messrs. Robert Davis and George Kollarek who assisted in the construction of the apparatus.

The authors also gratefully acknowledge the efforts of Mr. Robert Bergman who assisted in the preparation of the material used in the work herein described.

LIST OF FIGURES

Figures		Page
1.	Diagram of Apparatus	17
2a.	Front View of Apparatus	18A
2b.	Back View of Apparatus	18B
3.	Density vs. Percent Solids for Kaolin-Water Slurries . . .	21B
4.	Thermocouple Calibration	21C
5.	Kaolin Particle Size Distribution One Half Micron and Finer	21D
6.	Kaolin Particle Size Distribution Two Microns and Finer. .	21E
7.	Viscosity of 12.9% One Half Micron and Finer Kaolin Slurry	28
8.	Viscosity of 9.6% One Half Micron and Finer Kaolin Slurry.	29
9.	Viscosity of 5.6% One Half Micron and Finer Kaolin Slurry.	30
10.	Viscosity of 3.0% One Half Micron and Finer Kaolin Slurry.	31
11.	Viscosity of 23.1% Two Micron and Finer Kaolin Slurry. . .	32
12.	Viscosity of 20.4% Two Micron and Finer Kaolin Slurry. . .	33
13.	Viscosity of 13.7% Two Micron and Finer Kaolin Slurry. . .	34
14.	Viscosity of 10.1% Two Micron and Finer Kaolin Slurry. . .	35
15.	Correlation of Heat Transfer Data.	36
16.	Determination of Δtm	51

LIST OF TABLES

Table		Page
I	Tabulation of Original Data	21A
II	Tabulation of Experimental Results.	26
III	Tabulation of Shear Rate versus Viscosity	27

ABSTRACT

A total of 51 heat transfer runs were made. In the first 25 runs, slurries of half micron and finer kaolin at 3.0, 5.6, 9.6 and 12.9% solids were used. Slurries of two microns and finer kaolin at 10.1, 13.7, 20.4 and 23.1% solids were used in the remaining 26 runs.

The Reynolds Numbers ranged from 0.9 to 2,020 for the 51 runs.

The data was correlated by the following equation:

$$\frac{h_f}{C_b V_b \rho_b} \left(\frac{C_b \mu_b}{K_b} \right)^{2/3} = 0.70 \left(\frac{D V_b \rho_b}{\mu_b} \right)^{-2/3}$$

for an L/D ratio of 68.7.

This is essentially the accepted correlation for Newtonian fluids in laminar flow. The viscosity used for the slurries investigated was the apparent bulk viscosity obtained from measurements with a Fann V-G viscometer which gave shear rate versus viscosity data. The viscosity used was that at the same shear rate present in the heat exchanger.

INTRODUCTION

Since non-Newtonian slurries are becoming increasingly important systems in the chemical industries heat transfer data for such fluids are a growing necessity. Because most of the work done to date has been for non-Newtonian fluids in turbulent flow, this thesis deals with heat transfer coefficients in laminar flow.

One purpose of this research was to determine heat transfer coefficients for kaolin-water slurries in laminar flow. The clay industry is currently faced with great demands for products which will serve many new and diversified uses. These new demands mean modification of existing products by methods and processes which until now were unrelated to the industry. Consequently, a great lack of technological information on clay and clay-water systems exists. Heat transfer coefficients are engineering tools which will almost certainly be in demand in the very near future.

Another purpose of this research was to determine a correlation for heat transfer coefficients of non-Newtonian slurries in laminar flow and compare it with those correlations already established for Newtonian fluids. If the Newtonian correlations apply to non-Newtonian fluids or apply under certain circumstances, much difficult, complicated, and expensive measuring would be eliminated. Metzner, Vaughn, and Houghton have presented some data which suggests this is the case for solutions of Carbopol in water and carboxymethylcellulose in water. It was thought that data on suspensions as well as on solutions would be required before any general conclusions could be considered.

THEORY

In recent years heat transfer data have frequently been gathered and correlated for non-Newtonian slurries flowing in the turbulent regime. In many instances the approach has been to compare these data with the classical correlations for Newtonian fluids. By changing coefficients and exponents and adding new dimensionless groups, correlations have been arrived at which are similar in form to those for Newtonian fluids. However, little work has been done on non-Newtonian slurries in the laminar regime. It is, therefore, a purpose of this thesis to determine the applicability of correlations for Newtonian slurries in laminar flow.

Non-Newtonian fluids are defined as all fluids which do not exhibit a direct proportionality between shear stress and shear rate. Shear rate is the velocity gradient established between two planes within the fluid a distance (dr) apart when one of the planes moves with a velocity of (du) with respect to the other. The shear stress is the force required to move the plane at velocity (du) divided by the area of the plane. Mirich (5) in his three volumes on Rheology has compiled practical and theoretical aspects of many non-Newtonian fluids and processes involving non-Newtonian fluids of widespread importance.

Most rheologists (17) (6) (20) agree on a method of classification of non-Newtonian fluids which includes three major categories:

a. Time independent non-Newtonian fluids,

b. Time dependent non-Newtonian fluids,

c. Viscoelastic fluids.

Time independent non-Newtonian fluids are those for which the shear stress remains constant at a given shear rate regardless of the length of time for which the shear is applied. The shear stress of time dependent non-Newtonian fluids varies with time at a given shear rate until it too becomes constant. Some rheologists (4) place both these types of fluids in the same category, one being merely an extension of the other into the realm of measurable time. Viscoelastic fluids are those possessing viscose as well as elastic properties.

Several types of fluids are members of the time independent group. The most obvious are Newtonian fluids which can be considered special cases among the range of non-Newtonian fluids.

The simplest type of non-Newtonian fluids, in theory at any rate, is the Bingham plastic. Although several materials have been classified as Bingham plastics Otto and Metzner (14) as well as Roth and Rich (18) have demonstrated that most of them deviate from the direct proportionality between shear stress and shear rate when measurements are taken over wide ranges of shear rate. Such evidence questions the reality of any true Bingham plastics if shear rate range were extended even further.

Another type of time independent non-Newtonian fluids is dilatant fluids. With these fluids the ratio of shear stress to shear rate increases with increasing shear rate. When the flow rate of these materials is increased, their resistance to flow becomes greater. Consequently dilatant materials are seldom used in process equipment.

The most important type of time independent non-Newtonian fluids is the pseudoplastic fluids. These fluids are the opposite fluids in that the ratio of shear stress to shear rate decreases with increasing shear rate. The logaritmic plot of shear stress and shear rate is often a straight line over moderate ranges of shear rate. Therefore, Ostwald (13) proposed the following approximate relationship which was elaborated upon by Reiner (17):

$$\tau = k\dot{\gamma}^{n} \qquad \text{Equation (1)}$$

where (k) and (n) are constants for the particular fluid, and (n) lies between 0 and 1. Since the ratio of shear stress to shear rate is defined as apparent viscosity,

$$\mu = k\dot{\gamma}^{n-1} \qquad \text{Equation (2)}$$

Therefore, the logarithmic plot of apparent viscosity and shear rate should be a straight line with a negative slope from 0 to -1.

Mooney (11) in his classic paper on explicit formulas for slip and fluidity defines fluidity as the ratio of shear rate to shear stress. More simply it is the reciprocal of apparent viscosity. Mooney further defines the mean fluidity of the fluid in capillary viscometers, and, it may be assumed, in pipelines which there is laminar flow, as $(4E_f/\pi a^3)$ divided by the shear stress at the wall of the tube. In this relationship (E_f) is the efflux due to fluidity in units of volume per time and (a) is the radius of the tube in units of distance. $(4E_f/\pi a^3)$ can easily be converted to engineering terms of (8V/D) where (V) is the bulk velocity and (D) the tube diameter. Although Equation (2) is an approximate

equation in that (n) is not a true constant, for pseudoplastic materials (n) can only vary between 0 and 1. Consequently, there can only be one apparent viscosity for a given shear rate. Therefore, the mean fluidity, or inversely the mean apparent viscosity, of a fluid flowing through a tube in laminar flow can be found by any device which will give an apparent viscosity for a shear rate numerically equal to (8V/D).

The theoretical relation for heat transfer based on parabolic distribution of mass velocity and assuming uniform radial conduction of heat is given by the analytical equation (8).

$$\frac{h_a D}{K_b} = \frac{2wC_{pb}}{\pi K_b L} \frac{1-8\Psi(n_1)}{1+8\Psi(n_1)} \qquad \text{Equation (3)}$$

In this equation

$$\Psi(n_1) = 0.10238^{-14.627n_1} + 0.01220^{-89.22n_1} + 0.00237^{-212n_1} + \ldots . \qquad \text{Equation (4)}$$

in which (n_1) represents the group $\pi K_b L/4wC_{pb}$.

Equation (3) is extremely unwieldy and for values of $wCpb/KbL$ greater than 10 it is closely approximated by the empirical expression

$$\frac{h_a D}{K_b} = 1.75 \left(\frac{wC_{pb}}{K_b L}\right)^{1/3} = 1.62 \left(\frac{4wC_{pb}}{\pi K_b L}\right)^{1/3} \qquad \text{Equation (5)}$$

Fluids become non-Newtonian when their viscosity varies with shear rate or in the case of pipelines with mass velocity. It is conceivable that the property of viscosity may influence heat transfer to non-Newtonian fluids. Equation (5) contains no viscosity term. However, when the right side of the equation is multiplied by $(D\mu_b/D\mu_b)^{1/3}$ it may be written as

$$\frac{h_a D}{K_b} = 1.62 \left[\left(\frac{C_p \mu}{K}\right)_b \left(\frac{D}{L}\right)\left(\frac{D \rho_b V}{\mu_b}\right)\right]^{1/3} \qquad \text{Equation (6)}$$

For convenience this equation may be expressed in terms of the Reynold's number by dividing both sides of the equation by $(C_p \mu/K)_b^{1/3}$ $(D\rho_b V/\mu_b)$ and rearranging. The resulting equation is

$$\left(\frac{h}{C_{pb} V \rho_b}\right)\left(\frac{C_p \mu}{K}\right)_b^{-2/3} \left(\frac{D}{L}\right)^{1/3} = 1.62 \left(\frac{D \rho_b V}{\mu_b}\right)^{-2/3} \qquad \text{Equation (7)}$$

Any heat transfer data can be plotted with the Reynold's number as the abscissa and the groups $(h/C_{pb} V \rho_b)(C_p \mu/K)_b^{2/3}$ as the ordinate and compared with Equation (7).

LITERATURE SEARCH

A search was made of the available literature to determine progress already made by other investigators. It was noted that heat transfer to non-Newtonian fluids has only been studied for the past decade or two. However, non-Newtonian fluids as such have been under consideration since the 1920's.

Several methods of evaluating viscosities for heat transfer data have been used. Miller (10), Salamone and Newman (19), and Binder and Pollara (1) placed a pipe of dimensions identical to their heat exchanger in series with the exchanger. Pressure taps were installed in both ends of the pipe. The fluid leaving the heat exchanger was cooled to the average temperature of the fluid in the exchanger before entering the pipe. A curve relating the Reynolds number with the friction factor was made for this apparatus by calibrating it with a Newtonian fluid. When the non-Newtonian fluid was introduced to the system the pressure drop across the pipe was measured. This permitted the friction factor to be calculated and the corresponding Reynolds number to be determined. The only unknown in the Reynolds number was the viscosity which could then be easily calculated. This system has the advantage of measuring the fluid at exactly the same conditions of flow and temperature as exist in the heat exchanger. It also involves simple measurements and quick calculations. However, it is not too applicable to laminar flow. With flow rates low enough to insure laminar flow and pipe diameters large enough to insure a substantial heat transfer area the pressure drop across the viscometer section of the equipment is often too small to be measured.

Several investigators (2) (25) (10) (12) have used laboratory viscometers for the evaluation of the viscosities of the fluids in their heat transfer experiments. Of the types used the most prevalent is the capillary variety. One of the more elaborate capillary viscometers is the one designed by Orr and DallaValle (12). It was especially designed for suspensions of solids in liquids. It consists of a constantly agitated suspension reservoir in an oil bath. A capillary tube leads from the bottom of the reservoir to a receiving vessel upon which varying degrees of vacuum can be applied. The heating oil is caused to flow downward through an annulus surrounding most of the length of the capillary and upward through a return line to the main oil bath. Since the fluid is agitated up until the time it enters the capillary settling is minimized. This apparatus has the disadvantage of being limited to a maximum pressure differential of 14.7 psi. If this is not enough to cover the desired range of shear rates the diameter of the capillary must be changed. Changing the capillary tube is a cumbersome and time consuming task. A further disadvantage is the fact the fluid reservoir is open to the atmosphere. Most heat transfer experiments employ steam as the heat giving medium. Further, most suspensions of interest are those of solids in water. If the viscosity of the fluid in question at the temperature of the heat exchanger wall were attempted to be measured in this equipment, rapid vaporization or boiling would occur in the fluid reservoir thus changing the percent solids. Boiling would also occur in the capillary causing three phase flow. Therefore, the Sieder-Tate (21) correction factor of $(\mu/\mu_w)^{0.14}$ cannot be applied to heat transfer data obtained by experiments in which this method of viscosity evaluation is employed. This may not be serious

for often this correction lies within experimental error.

Metzner et al. (9) employed a capillary viscometer in which the fluid reservoir consisted of a closed vessel to which a pressure could be supplied. This eliminates the disadvantages of the Orr-DallaValle viscometer but provides no means of preventing settling of suspensions.

Among the many rotational viscometers a particularly suitable one for relatively low shear rates is the Fann V-G. It consists of a bob suspended by a torsion spring around which a cylinder rotates. The cylinder speed and consequently the shear rate can be switched instantaneously to any one of six different settings. The shear rate range from the lowest to the highest setting varies a hundred fold. Readings are almost instantaneous and are given directly in units of shear stress. The fluid reservoir in this apparatus, as indeed in all rotational viscometers, is open to the atmosphere. Therefore, the Sieder-Tate correction factor must again be neglected in experiments employing this type of viscometer. Lirich (5), Wilkinson (24), Green (6), and others describe many other types of viscometers which might be useful to a particular system.

Metzner et al. (9) presented experimental data on heat transfer coefficients of non-Newtonian fluids in laminar flow and compared them with the following theoretical relationships which they had derived:

$$\frac{hD}{K} = 1.75\,\delta^{1/3}\left(\frac{wC_p}{KL}\right)^{1/3} \qquad \text{Equation (8)}$$

$$\frac{hD}{K} = 1.75\,\Delta^{1/3}\left(\frac{wC_p}{KL}\right)^{1/3} \qquad \text{Equation (9)}$$

The choice between Equation (8) and Equation (9) depends on the range of Graetz numbers and flow behavior indices used. (The flow behavior index is approximately equal to (n) in Equation (1). The expression for (δ) and (Δ) were derived analytically, and the approach was based on the theoretical work of Pigford (16). It should be mentioned that, although the data agreed reasonably well with Equations (8) and (9), the agreement was no better than with the theoretical relationship for heat transfer coefficients of Newtonian fluids,

$$\frac{hD}{K} = 1.75 \left(\frac{wC_p}{KL}\right)^{1/3} \qquad \text{Equation (5)}$$

This raises some doubt as to the justification of including the (δ) or (Δ) factor particularly in work of an engineering nature. Metzner et al. brought the data into closer agreement with the theoretical curves by including the Sieder-Tate correction factor. However, this caused most of the data points to fall below the theoretical curve. This was explained by the fact that the input heat flux was used to determine the heat transfer coefficients. It may also be true that the Sieder-Tate correction factor does not apply exactly to non-Newtonian fluids whose viscosities are affected by not only the difference in temperature but also the difference in shear rate encountered at the tube wall.

Martinelli et al. (7) give the following analytical relationship for heating fluids flowing vertically upward and cooling fluids flowing vertically downward in laminar flow:

$$\frac{hD}{K} = 1.75\, F_1 \sqrt[3]{\frac{wC_p}{KL} + 0.0722\left[\frac{D}{L} N_{Gr}, N_{Pr}\right]_w^n}\, F_2 \qquad \text{Equation (10)}$$

The F factors and the quantity $0.0722\left[\ /L,\ N_{Gr}\ ,\ 1N_{Pr}\right]_{W}^{n}$ are included for natural convection. The material closest to the wall of the tube has a different temperature than the bulk of the fluid and consequently has a different density. This difference in density creates a buoyant force which increases the velocity of the fluid at the wall. However, Sieder (15) suggests that with fluids of high kinematic viscosities flowing in laminar flow through pipes of small diameter and having moderate temperature potentials the effect of natural convection becomes almost negligible compared to that of forced convection. When the effect of natural convection is neglected equation (10) reduces to equation (9).

Thermal conductivities of suspensions have been of considerable interest for several years. Maxwell (22) reasoned that the problem is exactly the same as that for electrical conductivity. He therefore wrote the thermal analog for Maxwell's equation for electrical conductivities as

$$k_b = k_1 \left[\frac{2K_1 + k_p - 2\phi_v (k_1 - k_p)}{2k_1 + k_p + \phi_v (k_1 - k_p)}\right] \qquad \text{equation (11)}$$

where k_b, k_1 and k_p are the thermal conductivities of the suspension, liquid and solid particles respectively and ϕ_v is the volume fraction of solids. He checked this equation with previously reported experimental data and found good agreement. Carr and Dallavalle (12) compared the equation with other experimental data and found excellent agreement. Carr and Dallavalle also measured the thermal conductivity of various suspensions. Their method of measurement was unique in that they added to the suspension to be measured two percent by weight agar gel in order to prevent settling during the tests. The data obtained by this method agreed with equation (11)

to within three percent.

Tsao (23) recently published an analytical approach to thermal conductivities of two phase materials. His final equation, however, is quite cumbersome and requires some experimental measurements. The value of this approach seems questionable in the light of the results of Tareef and Orr and DallaValle.

Description Of Apparatus

Figure I is a diagram of the apparatus. The details for each piece of equipment referred to on the diagram by a number are as follows:

1. Twenty gallon slurry storage tank.

2. Submerged type 3/8" vane pump with neoprene impeller driven by a 1/4 HP motor at 1725 RPM.

3. Experimental Heat Exchanger - Double annulus heat exchanger consisting of a 7' long, 1" schedule 40 red brass pipe inside a 6' long, 2", schedule 40 steel pipe and both inside a 6' long, 3", schedule 40 steel pipe. The inner annulus between the brass pipe and the 2" steel pipe was sealed by a packing box at each end. The boxes were made from 1 1/2" steel pipe couplings, 1 1/4" x 1 1/2" bushings and asbestos graphite packing. The outer annulus between the 2" and 3" steel pipes was sealed by welding the ends of the pipes together. A 3/4" steel pipe coupling served as the steam inlet to both jackets. A 1/2" steel pipe coupling was welded to both the 2" steel pipe and the 3" steel pipe on the other end of the heat exchanger to serve as condensate outlets from each jacket.

Six iron-constantan thermocouples (#24 wire), placed a foot apart and displaced clockwise 60°, were soldered halfway into the wall of the brass pipe to measure the temperature along the entire length of the pipe. The thermocouple wires, insulated with teflon, were brought out to the ends of the brass pipe (three at each end) by cementing them into a 3/16" wide x 0.133" deep x 2 1/2' long machine groove with litharge and glycerin.

The heat exchanger was well insulated to minimize heat losses.

4. Steam Calorimeter - Throttling type steam calorimeter to measure the quality of the steam going into the heat exchanger. An aspirator with a water cooled condenser maintained a partial vacuum on the low pressure side of the calorimeter.

5. Coolers - An annulus-type cooler consisting of a 9' long, 1" schedule 40 stainless steel pipe inside a 8' long, 1 1/2" schedule 40 steel pipe. The jacket was sealed by welding the ends of the outer pipe to the inner pipe. A 1/2" steel pipe coupling was welded at each end of the 1 1/2" pipe to serve as connections to the jacket.

6. Scale - Scale to weigh condensate from heat exchanger.

7. Two 1/2" bucket type steam traps.

8. Condensate Cooler - An annulus type cooler consisting of a 24" long, 1/2" schedule 40 steel pipe inside a 22" long, 1" schedule 40 steel pipe. The jacket was sealed by welding the ends of the outer pipe to the inner pipe. A 1/2" steel pipe coupling was welded at each end of the outer pipe to serve as connections to the jacket.

9. Thermometer - 0° to 100° C with 0.1° C subdivisions.

10. Slurry Mixing Valve.

11. Valve - Valve to control flow rate of slurry through apparatus.

The heat exchanger and the coolers were mounted vertically around and clamped to a 2" support pipe which was held firm by being fastened to the floor and the ceiling.

The slurry flowed upward through the heat exchanger.

The thermocouples were connected to a multipoint switch which was connected to a potentiometer.

A Fann rotational viscometer was used to measure the viscosities of the slurries. The viscometer consisted of a rotating cylinder around a bob supported by a torsion wire. The cylinder radius was 93/128 in. The bob had a radius of 87/128 in. and a height of 1.5 in. The torsion wire was connected mechanically to the instrument dial which read directly in pounds per 100 square feet. The cylinder rotated at speeds of 3, 6, 100, 200, 300 and 600 RPM and could be changed instantaneously while the instrument was running. Readings at all six speeds could be taken in less than a minute. Because of the speed of reading plus the very fine particles of the slurry, there was little or no settling during viscosity measurement.

Figures 2a and 2b are photographs of the apparatus.

DIAGRAM OF APPARATUS

FIGURE 1.

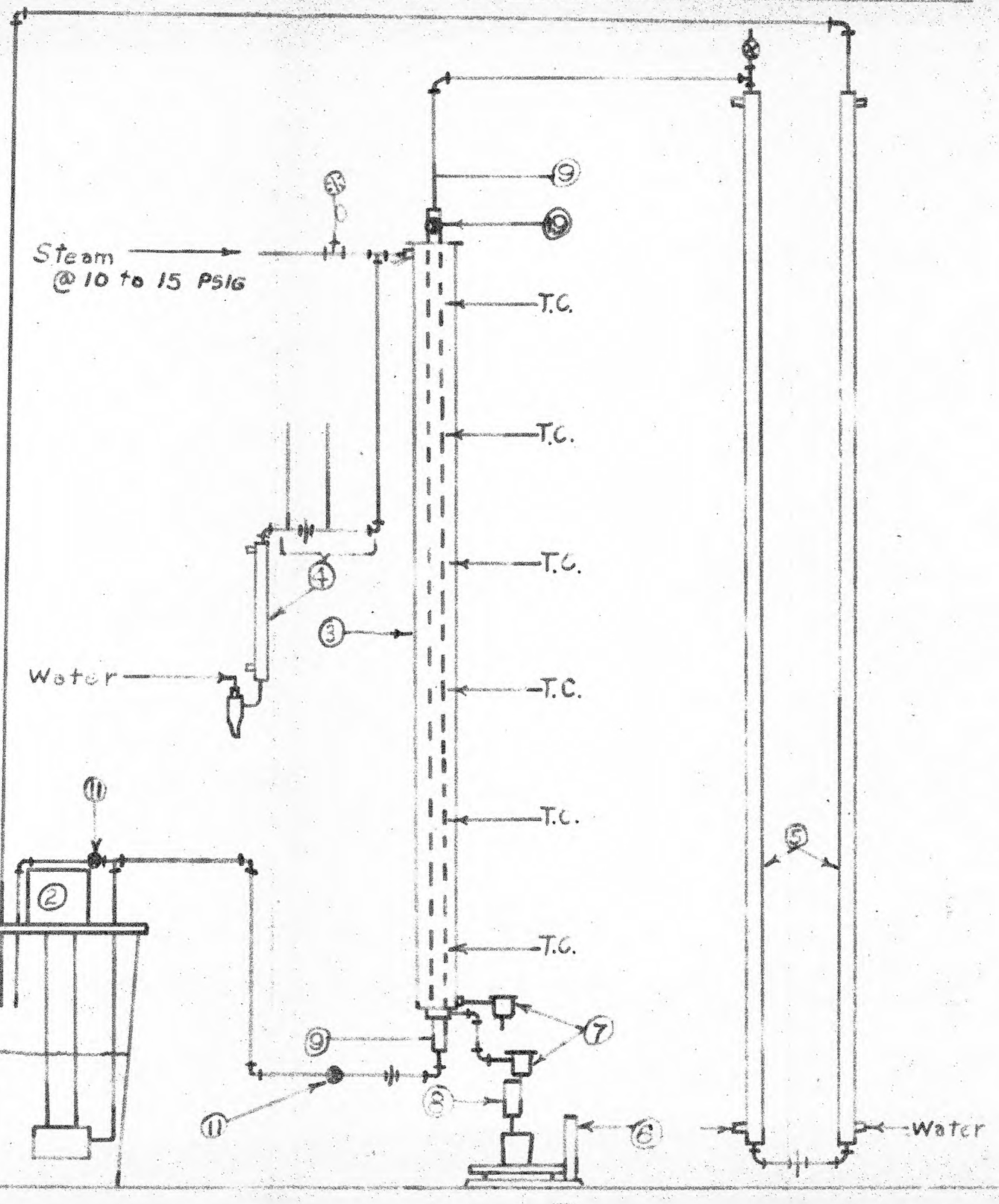

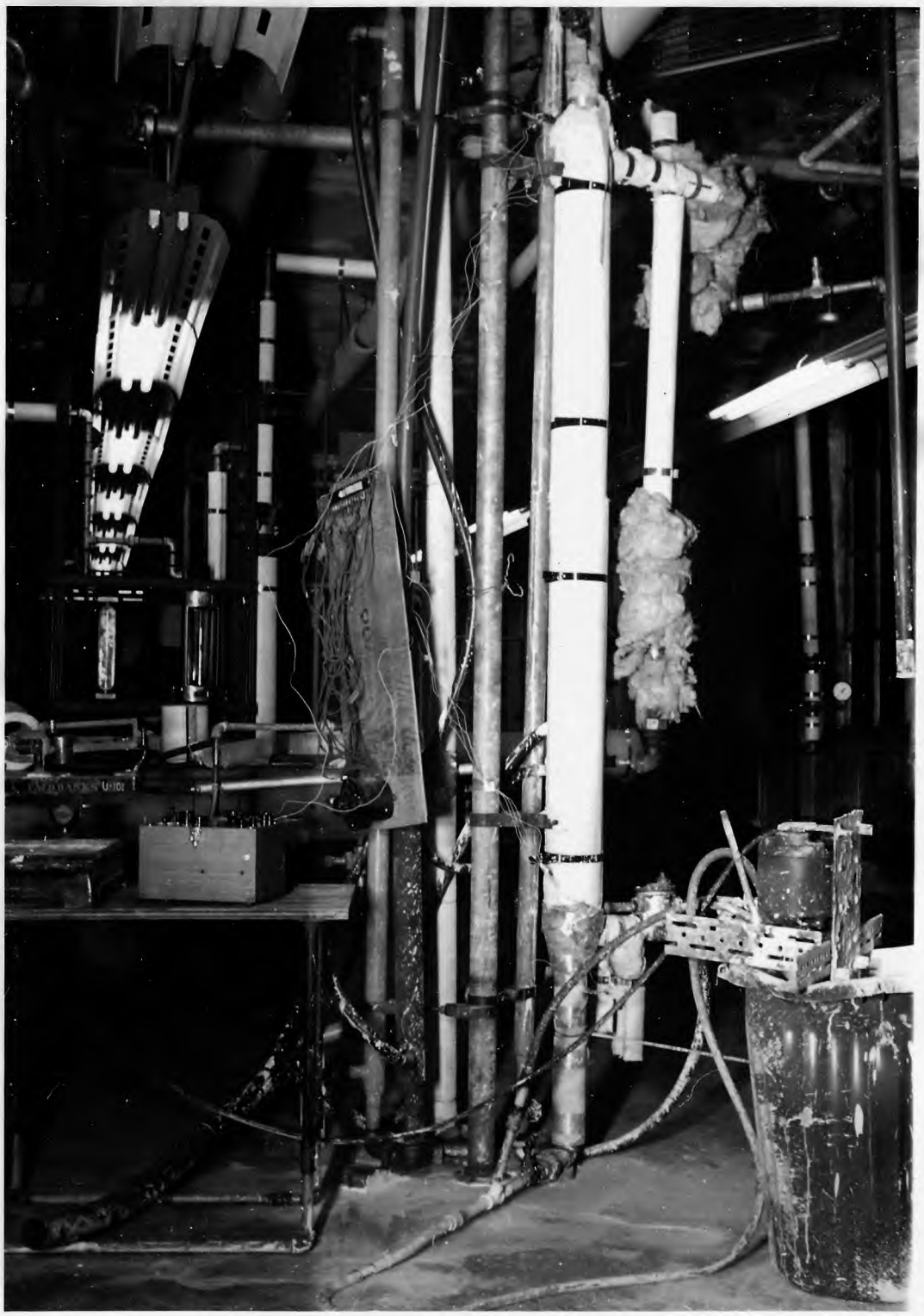

Figure 2a View of apparatus showing heat exchanger, coolers, potentiometer, multipoint thermocouple switch, and slurry storage tank with submerged circulating pump.

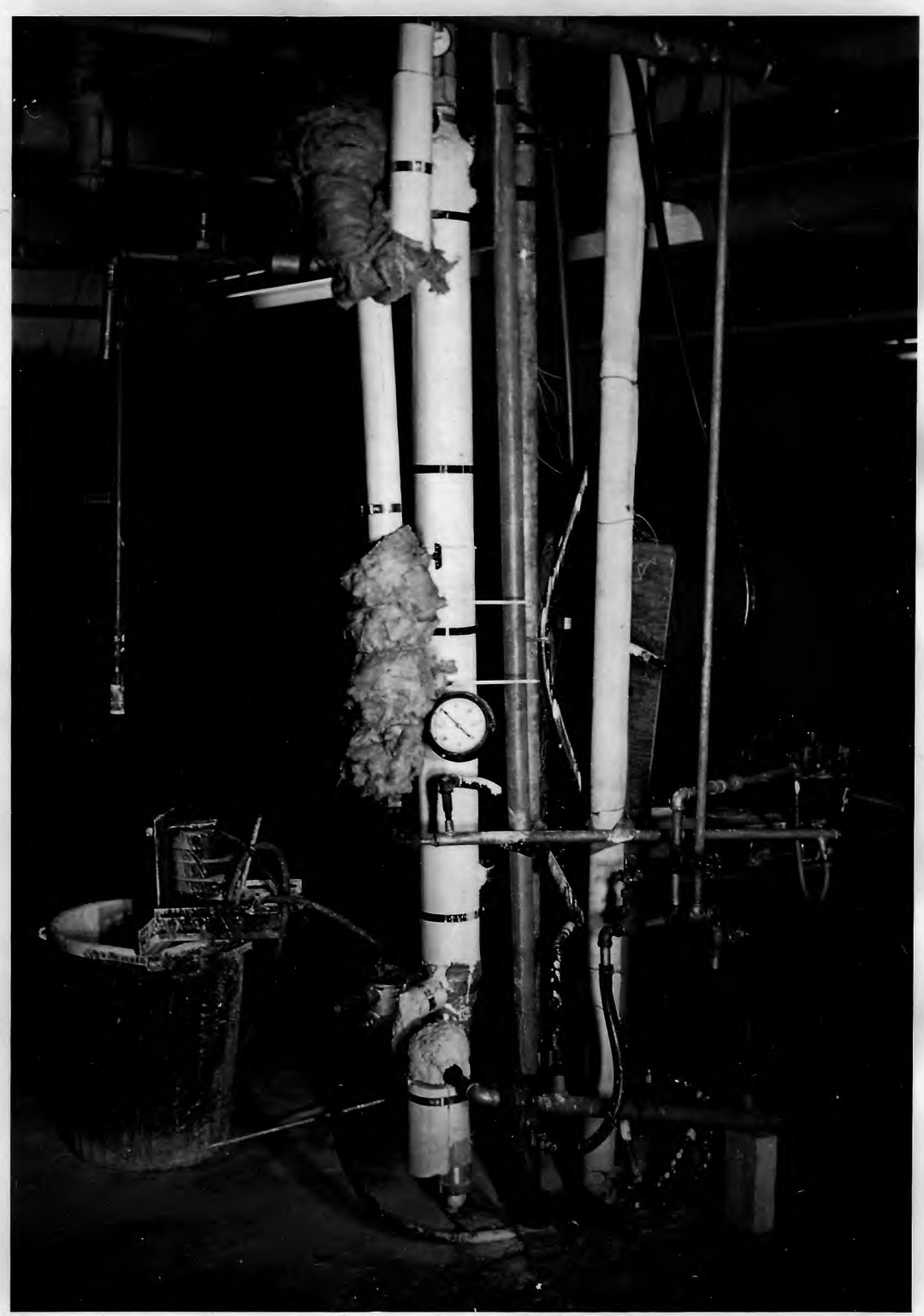

Figure 2b View of apparatus showing heat exchanger, coolers, steam calorimeter, condensate cooler, and slurry storage tank with submerged circulating pump.

Experimental Procedure

About a ten gallon batch of kaolin slurry was prepared by mixing the dry powder with water. The freshly prepared batch was made with the highest percentage of solids that was to be used. As experiments were made with the apparatus, the slurry was diluted with water to lower the solids content.

The apparatus was put into operation for collecting heat transfer data by starting the slurry circulating pump, turning on the tap water to all the coolers, turning on the steam and adjusting the steam pressure to about 10 to 15 psig, turning on the steam throttling calorimeter, connecting the potentiometer to the thermocouple switch, immersing the reference thermocouple junction into a dewar flask containing melting ice, and removing air from the slurry by opening the air vent valves.

The apparatus was allowed to run for a while at a high slurry flow rate (Reynolds number about 2,000) to let the temperatures of the slurry going into and coming out of the heat exchanger become constant. At this point, the apparatus was ready for taking data. The data that was taken is as follows: barometric pressure, temperature of the slurry going into and coming out of the heat exchanger, the six readings in millivolts of the thermocouples cemented into the brass pipe wall of the heat exchanger, temperatures and vacuum of the throttling calorimeter, heat exchanger condensate rate by taking a two, three, or four minute weight increment, steam inlet pressure to the heat exchanger, and rate of slurry flowing through the apparatus by taking a one-half, one, or two minute weight increment.

After the data for a run was taken, the slurry flow rate was reduced by about 15 to 20% by adjusting the two slurry rate control valves. Again the apparatus was allowed to run for a while, letting the temperatures of the slurry going into and coming out of the heat exchanger become constant. At this point, data for another run was taken. This procedure was followed for about six or seven runs, then the concentration of solids in the slurry was reduced by removing about 15 to 30% of the slurry from the batch and replacing it with water. After the slurry was thoroughly mixed, the procedure, outlined above, was repeated.

The apparatus was shut down by first turning off the steam, turning off the water to the coolers, stopping the slurry circulating pumps, and disconnecting the potentiometer.

A sample was taken from each batch of slurry. After each sample was checked for percent solids, viscosity runs were made with a Fann viscometer. Viscometer speeds of 3, 6, 100, 200, 300 and 600 rpm were made on the slurry at the average temperature the slurry was at in the heat exchanger. The shear stress at each of these viscometer speeds was recorded.

A total of 51 runs were made with the apparatus. A 1/2 micron and finer kaolin was used in the first 25 runs. The remaining 26 runs were made with a 2 micron and finer kaolin.

Table I is a tabulation of the original data. Figure 3 is a plot of slurry density versus percent kaolin in water. Figure 4 is a plot of degrees fahrenheit versus millivolts for iron-constantan thermocouple.

Figure 5 is a particle size distribution curve of 1/2 micron and finer kaolin. Figure 6 is a particle size distribution curve of 2 micron and finer kaolin.

TABLE I

TABULATION OF ORIGINAL DATA

	Run No. 1	Run No. 2	Run No. 3	Run No. 4	Run No. 5	Run No. 6	Run No. 7	Run No. 8	Run No. 9	Run No
Fluid Inlet Temp. M.V.	1.48	1.50	1.46	1.47	1.47	1.47	1.43	1.19	1.39	1.48
Ex. Wall Temp. #2 M.V.	6.02	5.97	6.00	6.01	6.09	5.75	5.78	5.93	5.92	5.96
Ex. Wall Temp. #3 M.V.	6.35	6.19	6.30	6.35	6.39	5.39	5.85	6.12	6.13	6.13
Ex. Wall Temp. #4 M.V.	6.30	6.18	6.15	6.10	6.30	5.93	5.94	6.11	6.10	6.15
Ex. Wall Temp. #5 M.V.	6.03	5.92	6.02	6.10	6.10	5.77	5.71	5.78	5.85	5.89
Ex. Wall Temp. #6 M.V.	6.30	6.20	6.28	6.35	6.31	5.93	5.93	6.10	6.11	6.15
Ex. Wall Temp. #7 M.V.	6.37	6.23	6.32	6.35	6.37	5.98	5.93	6.14	6.16	6.15
Fluid Outlet Temp. #8 M.V.	1.90	1.90	2.00	2.14	2.32	3.12	2.64	1.62	1.81	2.03
Fluid Mass Rate	11 3/8 lb/30 sec	9 1/4 lb/30 sec	7 3/16 lb/30 sec	5 lb/30 sec	3 9/16 lb/30 sec	1 1/8 lb/30 sec	3 5/16 lb/min	12 5/16 lb/30 sec	10 11/16 lb/30 sec	8 1/8 lb/
Steam Inlet Pressure, PSIG	14.0	11.6	12.7	13.7	13.8	7.7	7.3	9.7	10.5	10.4
Steam Mass Rate	530 grm/4 min	351 grm/3min	327 grm/3 min	308 grm/3 min	293 grm/3 min	229grm/4 min	259 grm/4 min	477 grm/3 min	437 grm/3 min	404 grm/3
Orifice Upstream Temp., °F	246	242	244	246	246	232	232	238	239	238
Orifice Downstream Temp., °F	180	175	177	178	177	168	166	171	171	170
Orifice Downstream Vacuum, In. Hg.	15.7	17.1	16.4	15.8	15.7	19.0	19.7	18.3	18.4	18.2
% Solids	12.9	12.9	12.9	12.9	12.9	12.9	12.9	9.6	9.6	9.6
Barometric Pressure, In. Hg.	29.65	29.65	29.65	29.65	29.65	29.65	29.65	29.65	29.65	29.65
Fann Viscometer Data:										
Avg. Temp. °F	90.5	90.8	91.6	94.3	90.4	115.4	102.2	82.1	89.1	92.6
lb/100 ft² @ 3 RPM	13.5	13.5	13.5	13.2	13.5	12.5	13.5	7.5	6.7	6.7
lb/100 ft² @ 6 RPM	17.0	17.0	17.0	17.2	17.0	16.5	18.0	8.5	7.5	7.5
lb/100 ft² @ 100 RPM	26.7	26.7	26.7	27.5	26.7	27.2	27.6	11.8	11.5	11.5
lb/100 ft² @ 200 RPM	29.8	29.8	29.8	30.0	29.8	29.7	30.0	13.7	13.2	13.2
lb/100 ft² @ 300 RPM	31.5	31.5	31.5	31.5	31.5	30.5	31.5	16.2	14.7	14.7
lb/100 ft² @ 600 RPM	36.5	36.5	36.5	36.2	36.5	35.2	36.0	19.8	18.5	18.5

	Run No. 8	Run No. 9	Run No. 10	Run No. 11	Run No. 12	Run No. 13	Run No. 14	Run No. 15	Run No. 16	Run No. 17	Run No. 18	Run No. 19	
	1.19	1.39	1.48	1.48	1.58	1.50	1.48	1.13	1.46	1.55	1.58	1.58	
	5.93	5.92	5.96	5.93	5.83	5.89	5.82	5.91	5.90	5.95	5.85	5.99	
	6.12	6.13	6.13	6.15	6.00	6.12	6.04	6.09	6.11	6.10	5.98	6.20	
	6.11	6.10	6.15	6.14	6.01	6.08	6.00	6.10	6.08	6.11	6.00	6.18	
	5.78	5.85	5.89	5.89	5.65	5.90	5.82	5.77	5.80	5.78	5.70	6.00	
	6.10	6.11	6.15	6.13	6.00	6.08	6.00	6.11	6.10	6.11	5.98	6.16	
	6.14	6.16	6.15	6.18	6.00	6.08	6.00	6.11	6.10	6.11	6.10	6.20	
	1.62	1.81	2.03	2.19	2.4[illegible]	4.10	3.38	1.62	2.02	2.33	2.61	4.30	
in	12 5/16 lb/30 sec	10 11/16 lb/30 sec	8 1/8 lb/30 sec	6 1/8 lb/30 sec	7 3/8 lb/min	1 3/4 lb/min	2 1/2 lb/min	12 1/2 lb/30 sec	10 1/4 lb/30 sec	7 lb/30 sec	4 1/8 lb/30 sec	2 1/8 lb/65 sec	4
	9.7	10.5	10.4	10.6	8.2	9.3	9.1	10.0	10.6	10.2	8.2	10.8	
in	477 grm/3 min	437 grm/3 min	404 grm/3 min	368 grm/3 min	313 grm/3 min	209 grm/3 min	248 grm/3 min	622 grm/3 min	566 grm/3 min	513 grm/3 min	394 grm/3 min	246 grm/3 min	35
	238	239	238	240	236	236	235	238	239	239	234	240	
	171	171	170	171	169	169	169	169	170	170	165	170	
	18.3	18.4	18.2	18.1	18.8	18.8	18.9	18.8	18.5	18.5	20.0	18.5	
	9.6	9.6	9.6	9.6	9.6	9.6	9.6	5.6	5.6	5.6	5.6	5.6	
	29.65	29.65	29.65	29.65	29.65	29.65	29.65	29.65	29.65	29.65	29.65	29.65	
	82.1	89.1	92.6	95.4	100.0	128.0	119.2	82.5	93.4	100.2	104.0	132.7	
	7.5	6.7	6.7	6.7	7.0	7.2	6.8	1.5	2.0	2.0	2.0	1.5	
	8.5	7.5	7.5	7.5	8.0	8.5	8.0	2.0	2.2	2.0	2.0	2.2	
	11.8	11.5	11.5	11.5	11.5	11.5	11.2	3.5	3.5	3.5	3.5	3.5	
	13.7	13.2	13.2	13.2	13.2	12.5	12.8	5.0	4.8	4.7	4.7	4.2	
	16.2	14.7	14.7	14.7	14.5	13.5	13.2	5.5	5.5	5.5	5.5	4.8	
	19.8	18.5	18.5	18.5	17.5	16.5	16.5	8.0	7.5	7.2	7.2	6.0	

Run No. 16	Run No. 17	Run No. 18	Run No. 19	Run No. 20	Run No. 21	Run No. 22	Run No. 23	Run No. 24	Run No. 25	Run No. 26	Run No. 27
1.46	1.55	1.58	1.58	1.56	1.20	1.41	1.51	1.61	1.60	*35.4 °C	34.7 °C
5.90	5.95	5.85	5.99	5.79	5.80	5.95	5.89	5.98	5.99	5.90	6.05
6.11	6.10	5.98	6.20	5.90	6.09	6.12	6.10	6.10	6.18	6.10	6.20
6.08	6.11	6.00	6.18	5.92	6.06	6.10	6.08	6.10	6.17	6.09	6.19
5.80	5.78	5.70	6.00	5.67	5.70	5.79	5.77	5.81	5.95	5.90	6.00
6.10	6.11	5.98	6.16	5.91	6.07	6.10	6.09	6.10	6.15	6.10	6.18
6.10	6.11	6.10	6.20	5.96	6.07	6.10	6.09	6.10	6.20	6.10	6.21
2.02	2.33	2.61	4.30	3.28	1.83	2.34	2.63	3.87	4.70	45.5 °C	52.0 °C
10 1/4 lb/30 sec	7 lb/30 sec	4 1/8 lb/30 sec	2 1/8 lb/65 sec	4 7/16 lb/min	13 5/16 lb/30 sec	8 5/16 lb/30 sec	7 1/4 lb/30 sec	4 13/16 lb/min	3 lb/min	11 1/2 lb/30 sec	6 1/16 lb/min
10.6	10.2	8.2	10.8	7.5	10.6	11.0	10.2	10.1	11.1	13.8	12.6
566 grm/3 min	513 grm/3 min	394 grm/3 min	246 grm/3 min	354 grm/3 min	563 grm/2 min	499 grm/2 min	486 grm/2 min	358 grm/2 min	310 grm/2 min	519 grm/3 min	266 grm/2.5 min
239	239	234	240	232	239	240	240	238	240	243	241
170	170	165	170	165	170	170	170	168	170	127	126
18.5	18.5	20.0	18.5	19.9	18.7	18.5	18.7	19.0	18.4	25.5	25.4
5.6	5.6	5.6	5.6	5.6	3.0	3.0	3.0	3.0	3.0	23.1	23.1
29.65	29.65	29.65	29.65	29.65	29.65	29.65	29.65	29.65	29.65	29.54	29.54
93.4	100.2	104.0	132.7	114.9	86.9	98.9	102.6	125.7	139.6	104.9	110.3
2.0	2.0	2.0	1.5	1.8	0.2	0.2	0.2	0.2	0.2	13.5	13.5
2.2	2.0	2.0	2.2	2.2	0.5	0.5	0.5	0.5	0.5	17.7	17.7
3.5	3.5	3.5	3.5	3.5	1.3	1.2	1.2	1.2	1.2	30.1	30.1
4.8	4.7	4.7	4.2	4.5	2.0	1.7	1.7	1.7	1.7	34.0	34.0
5.5	5.5	5.5	4.8	5.0	2.5	2.2	2.2	2.0	2.0	36.9	36.9
7.5	7.2	7.2	6.0	6.5	3.8	3.5	3.5	3.0	3.0	41.9	41.9

* 0° 100°C Thermometer used instead of thermocouple - Runs 26 through Runs 51

TABLE I (cont.)

TABULATION OF ORIGINAL DATA

	Run No. 28	Run No. 29	Run No. 30	Run No. 31	Run No. 32	Run No. 33	Run No. 34	Run No. 35	Run No. 36	Run
Fluid Inlet Temp. M.V.	33.3 °C	32.6 °C	32.9 °C	32.6 °C	37.0 °C	37.0 °C	36.3 °C	35.4 °C	34.8 °C	34.
Ex. Wall Temp. #2 M.V.	6.10	5.83	5.75	5.77	5.81	5.73	5.72	5.83	5.88	5.
Ex. Wall Temp. #3 M.V.	6.29	5.98	5.90	5.91	6.02	6.00	5.95	6.08	6.10	5.
Ex. Wall Temp. #4 M.V.	6.25	6.01	5.94	5.90	6.00	5.90	5.90	6.00	6.00	5.
Ex. Wall Temp. #5 M.V.	6.07	5.77	5.70	5.69	5.80	5.80	5.80	5.88	5.91	5.
Ex. Wall Temp. #6 M.V.	6.22	6.02	5.95	5.91	6.00	5.91	5.90	6.00	6.00	5.
Ex. Wall Temp. #7 M.V.	6.29	6.02	5.95	5.90	5.95	5.89	5.90	6.00	6.00	5.
Fluid Outlet Temp. #8 M.V.	60.8 °C	46.5 °C	44.2 °C	49.0 °C	47.0 °C	49.3 °C	49.0 °C	51.2 °C	57.1 °C	44.
Fluid Mass Rate	10 lb/2 min	13 7/8 lb/min	9 3/8 lb/30 sec	9 5/8 lb/min	11 7/8 lb/30 sec	8 1/4 lb/30 sec	12 1/2 lb/min	9 1/2 lb/min	10 1/2 lb/2 min	12 lb/3
Steam Inlet Pressure, PSIG	14.0	10.1	9.0	8.5	9.2	8.5	8.0	9.0	9.5	7.
Steam Mass Rate	245 grm/2.5 min	269 grm/2 min	301 grm/2 min	228 grm/2 min	342 grm/2 min	273 grm/2 min	245 grm/2 min	222 grm/2 min	183 grm/2 min	324 grm
Orifice Upstream Temp., °F	239	238	232	231	236	234	233	236	237	23
Orifice Downstream Temp., °F	121	-	152	152	152	150	148.5	150	151	14
Orifice Downstream Vacuum, In. Hg.	25.5	25.6	22.5	23.0	23.2	23.6	23.9	23.6	23.5	23.
% Solids	23.1	23.1	23.1	23.1	20.4	20.4	20.4	20.4	20.4	20.
Barometric Pressure, In.Hg.	29.54	29.54	29.54	29.54	29.60	29.60	29.60	29.60	29.60	29.
Fann Viscometer Data:										
Avg. Temp., °F	116.6	103.1	101.3	101.3	107.6	109.6	108.8	109.9	114.6	103.
lb/100 ft² @ 3 RPM	9.0	13.0	13.5	13.5	10.0	10.0	10.0	10.0	10.0	10.
lb/100 ft² @ 6 RPM	17.5	18.0	17.7	17.7	12.0	12.0	12.0	12.0	12.0	12.
lb/100 ft² @ 100 RPM	29.0	30.0	30.1	30.1	19.4	19.4	19.4	19.4	19.2	20.
lb/100 ft² @ 200 RPM	33.0	33.5	34.0	34.0	22.1	22.1	22.1	22.1	22.0	22.
lb/100 ft² @ 300 RPM	35.5	36.2	36.9	36.9	24.1	24.1	24.1	24.1	23.5	24.
lb/100 ft² @ 600 RPM	40.2	41.0	41.9	41.9	28.0	28.0	28.0	28.0	27.5	28.

(cont.)

NAL DATA

n No. 34	Run No. 35	Run No. 36	Run 37	Run No. 38	Run No. 39	Run No. 40	Run No. 41	Run No. 42	Run No. 43	Run No. 44	Run No. 45	Ru
36.3 °C	35.4 °C	34.8 °C	34.8 °C	35.9 °C	33.4 °C	35.5 °C	39.4 °C	40.1 °C	40.0 °C	37.8 °C	31.0 °C	3
5.72	5.83	5.88	5.65	5.70	5.89	5.83	5.81	5.96	5.88	5.60	5.77	
5.95	6.08	6.10	5.90	5.90	6.16	6.00	5.98	6.17	6.17	5.84	5.94	
5.90	6.00	6.00	5.83	5.88	6.08	6.00	6.00	6.14	6.07	5.75	5.96	
5.80	5.88	5.91	5.71	5.71	5.92	5.81	5.88	6.00	6.02	5.75	5.74	
5.90	6.00	6.00	5.81	5.86	6.07	5.93	5.93	6.08	6.09	5.75	5.88	
5.90	6.00	6.00	5.85	5.90	6.10	6.01	6.02	6.20	6.20	5.85	6.00	
49.0 °C	51.2 °C	57.1 °C	44.4 °C	46.5 °C	44.5 °C	50.0 °C	51.7 °C	62.3 °C	65.5 °C	52.4 °C	42.4 °C	1
1/2 lb/min	9 1/2 lb/min	10 1/2 lb/2 min	12 lb/30 sec	9 7/8 lb/30 sec	12 1/4 lb/30 sec	8 3/8 lb/30 sec	10 1/4 lb/30 sec	9 lb/min	9 5/8 lb/ 1 1/2 min	13 3/8 lb/min	12 1/2 lb/30 sec	10
8.0	9.0	9.5	7.0	7.7	11.7	9.1	9.5	11.5	11.5	6.6	8.6	1
5 grm/2 min	222 grm/2 min	183 grm/2 min	324 grm/2 min	299 grm/2 min	209 grm/min	185 grm/min	196 grm/min	166 grm/min	135 grm/min	299 grm/2 min	446 grm/2 min	451
233	236	237	230	232	240	236	236	241	241	230	235	
148.5	150	151	149	148	158	140	139	142	140	135	95.5	
23.9	23.6	23.5	23.8	24.0	22.0	25.4	25.5	25.2	25.5	26.2	29.4	
20.4	20.4	20.4	20.4	20.4	13.7	13.7	13.7	13.7	13.7	13.7	10.1	
29.60	29.60	29.60	29.60	29.60	29.93	27.93	29.93	29.93	29.93	29.93	29.98	
108.8	109.9	114.6	103.3	106.1	102.2	109.0	114.1	125.6	128.0	113.1	98.0	
10.0	10.0	10.0	10.0	10.0	4.1	4.1	4.0	3.8	3.8	4.0	1.3	
12.0	12.0	12.0	12.5	12.3	4.5	4.4	4.3	4.2	4.2	4.3	1.8	
19.4	19.4	19.2	20.0	19.7	6.2	6.1	6.0	5.2	5.2	6.0	3.1	
22.1	22.1	22.0	22.3	22.2	7.5	7.3	7.2	6.9	6.9	7.2	4.1	
24.1	24.1	23.5	24.5	24.3	8.8	8.3	8.1	7.9	7.9	8.1	4.9	
28.0	28.0	27.5	28.7	28.3	10.9	10.3	10.1	9.3	9.3	10.1	6.8	

Run No. 42	Run No. 43	Run No. 44	Run No. 45	Run No. 46	Run No. 47	Run No. 48	Run No. 49	Run No. 50	Run No. 51
40.1 °C	40.0 °C	37.8 °C	31.0 °C	33.1 °C	34.5 °C	35.9 °C	34.7 °C	34.5 °C	33.7 °C
5.96	5.88	5.60	5.77	5.70	5.73	5.72	5.71	5.76	5.73
6.17	6.17	5.84	5.94	5.96	6.05	6.03	5.88	5.98	5.95
6.14	6.07	5.75	5.96	5.87	5.89	5.88	5.90	5.95	5.94
6.00	6.02	5.75	5.74	5.83	5.85	5.85	5.70	5.81	5.74
6.08	6.09	5.75	5.88	5.90	6.00	6.00	5.84	5.90	5.89
6.20	6.20	5.85	6.00	6.00	6.11	6.08	5.94	6.05	5.99
62.3 °C	65.5 °C	52.4 °C	42.4 °C	46.2 °C	49.7 °C	52.9 °C	44.4 °C	50.4 °C	43.5 °C
9 lb/min	9 5/8 lb/ 1 1/2 min	13 3/8 lb/min	12 1/2 lb/30 sec	10 lb/30 sec	7 lb/30 sec	12 lb/min	11 3/8 lb/30 sec	7 lb/30 sec	12 1/8 lb/30 sec
11.5	11.5	6.6	8.6	10.0	10.4	9.6	8.0	9.0	8.1
166 grm/min	135 grm/min	299 grm/2 min	446 grm/2 min	451 grm/2 min	355 grm/2 min	342 grm/2 min	347 grm/2 min	353 grm/2 min	374 grm/2 min
241	241	230	235	236	239	237	233	235	234
142	140	135	95.5	86	150.5	141	137	139	138
25.2	25.5	26.2	29.4	29.6	23.6	25.3	25.8	25.6	25.7
13.7	13.7	13.7	10.1	10.1	10.1	10.1	10.1	10.1	10.1
29.93	29.93	29.93	29.98	29.98	29.98	29.98	29.98	29.98	29.98
125.6	128.0	113.1	98.0	103.4	107.8	111.9	103.2	108.4	101.4
3.8	3.8	4.0	1.3	1.3	1.2	1.2	1.3	1.2	1.3
4.2	4.2	4.3	1.8	1.7	1.6	1.5	1.7	1.6	1.8
5.2	5.2	6.0	3.1	3.1	3.1	3.0	3.1	3.1	3.1
6.9	6.9	7.2	4.1	4.1	4.1	3.9	4.1	4.1	4.1
7.9	7.9	8.1	4.9	4.7	4.6	4.3	4.7	4.6	4.9
9.3	9.3	10.1	6.8	6.3	6.1	5.9	6.3	6.1	6.8

FIGURE 3

DENSITY OF KAOLIN SLURRY

Density vs. Portent Kaolin

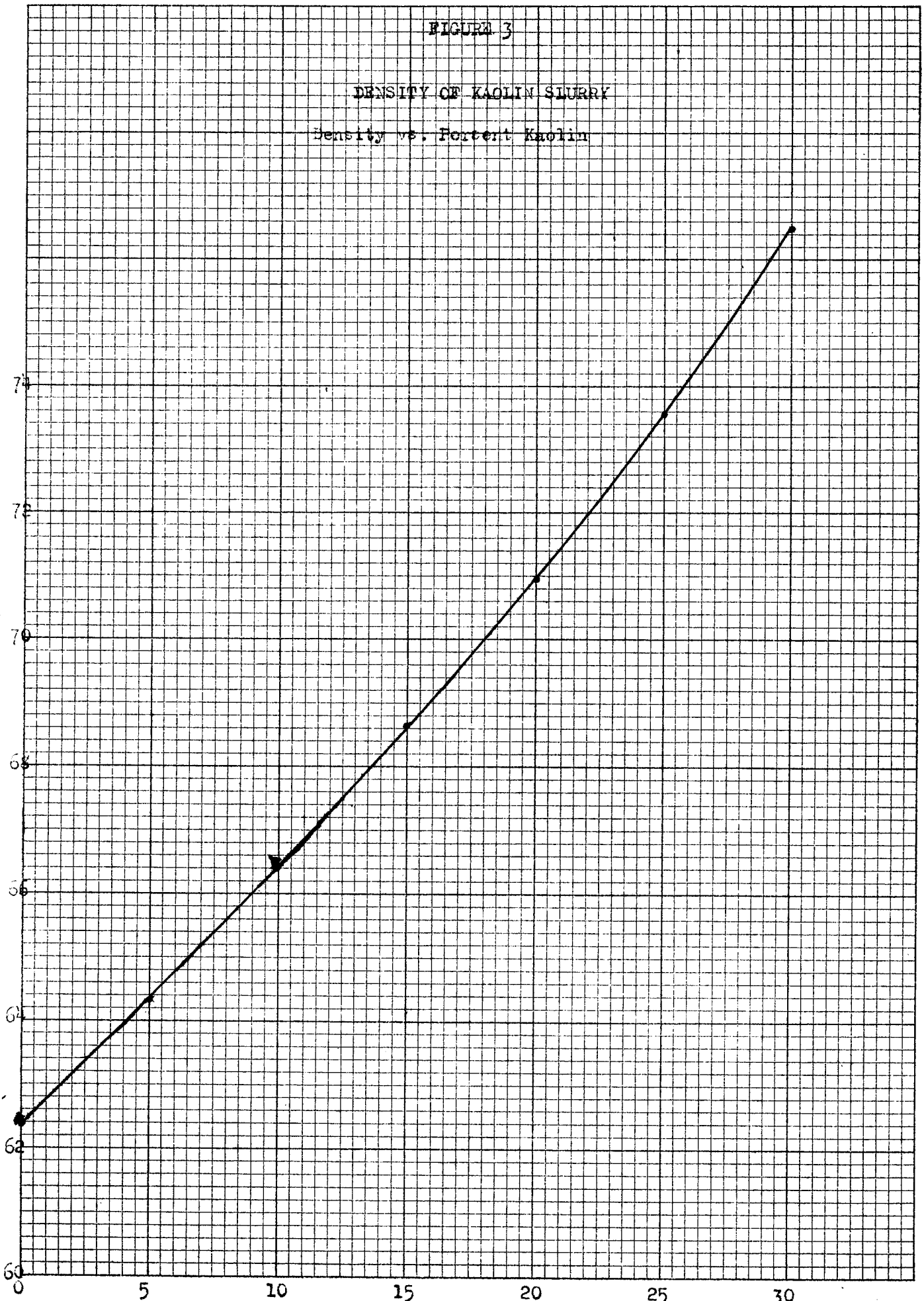

FIGURE 4

THERMOCOUPLE CALIBRATION
(Iron Constantan)

Degrees Fahrenheit vs. millivolts

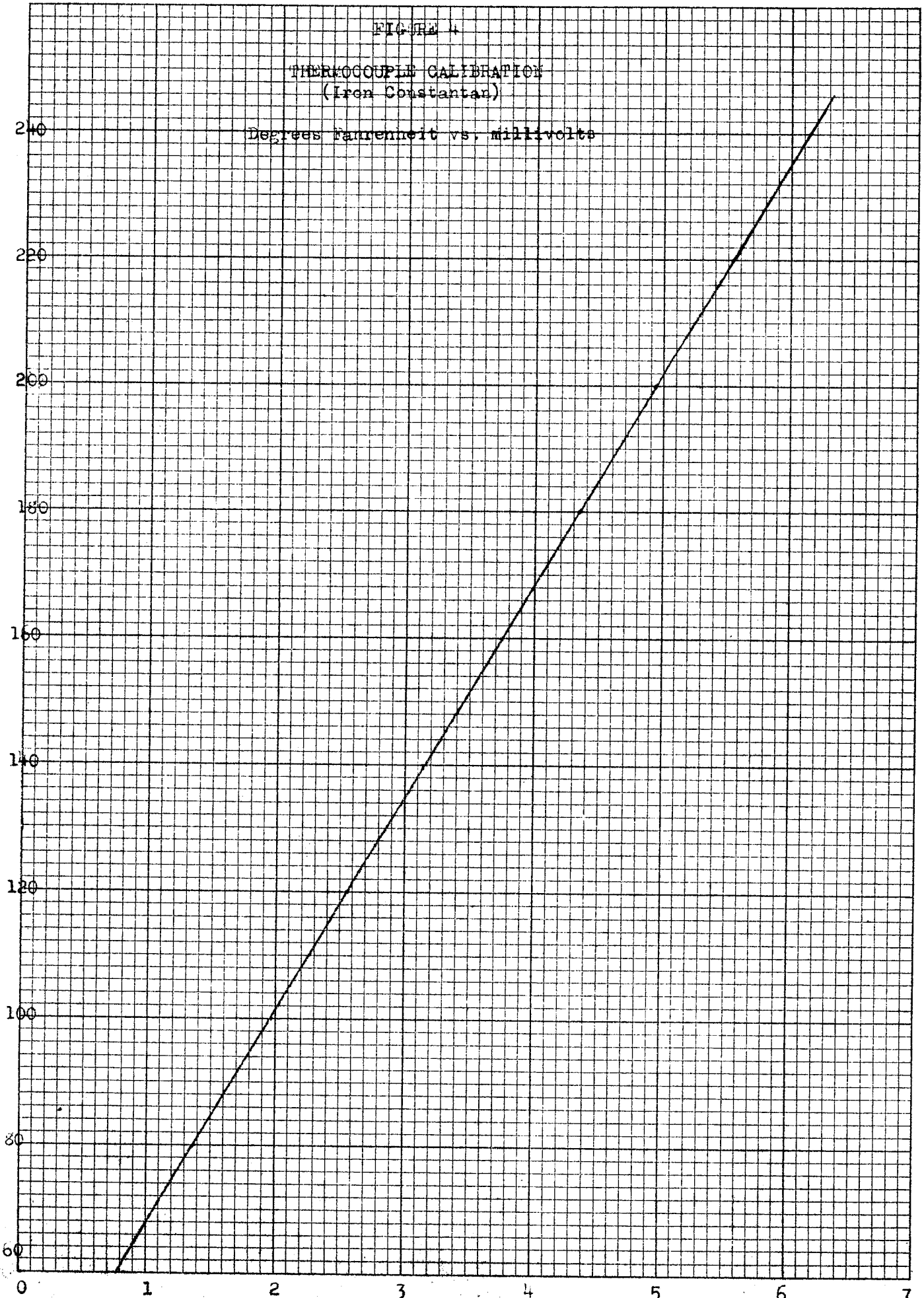

FIGURE 5

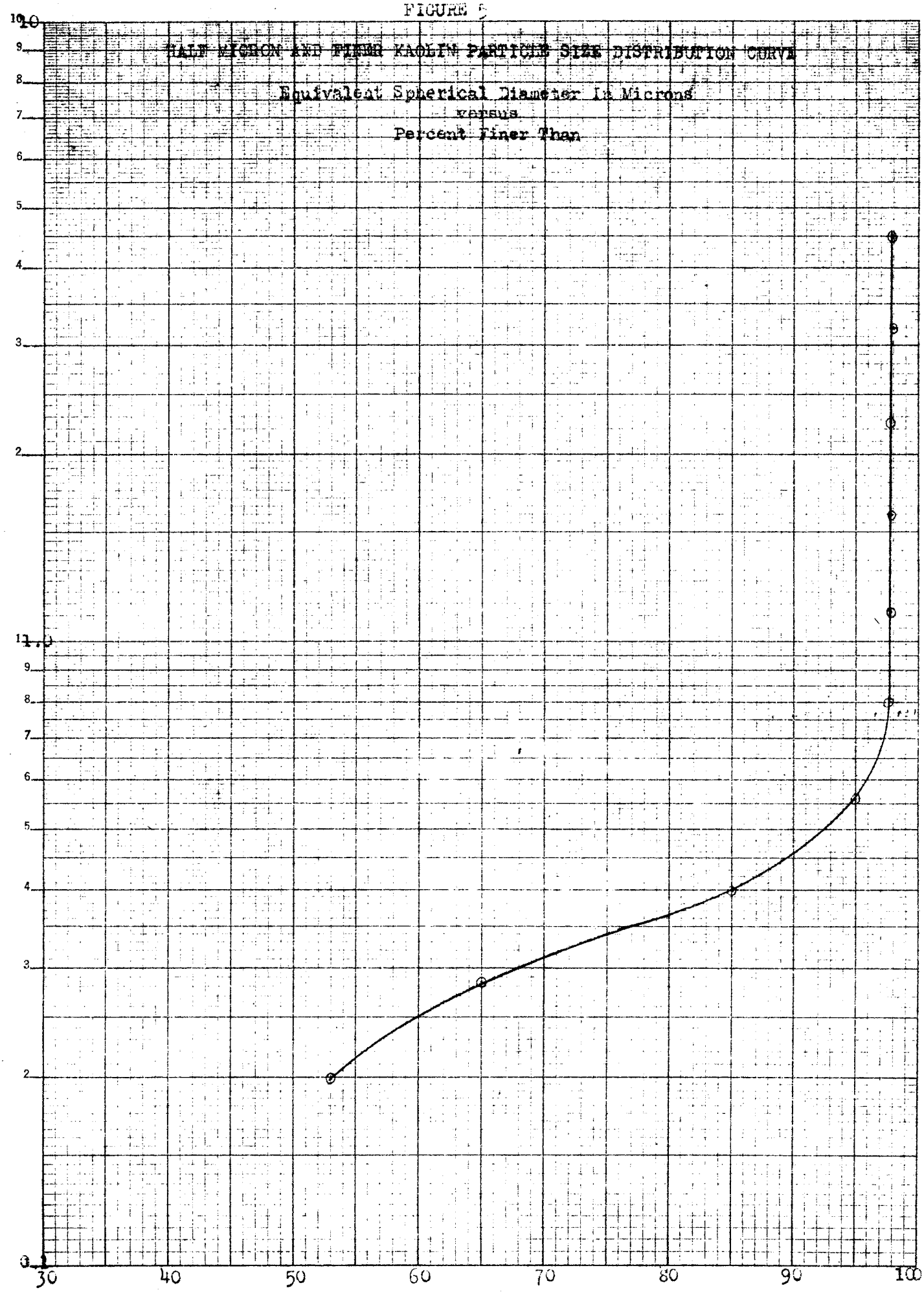

FIGURE 6

TWO MICRON AND FINER KAOLIN PARTICLE SIZE DISTRIBUTION CURVE

Equivalent Spherical Diameter In Microns
versus
Percent Finer Than

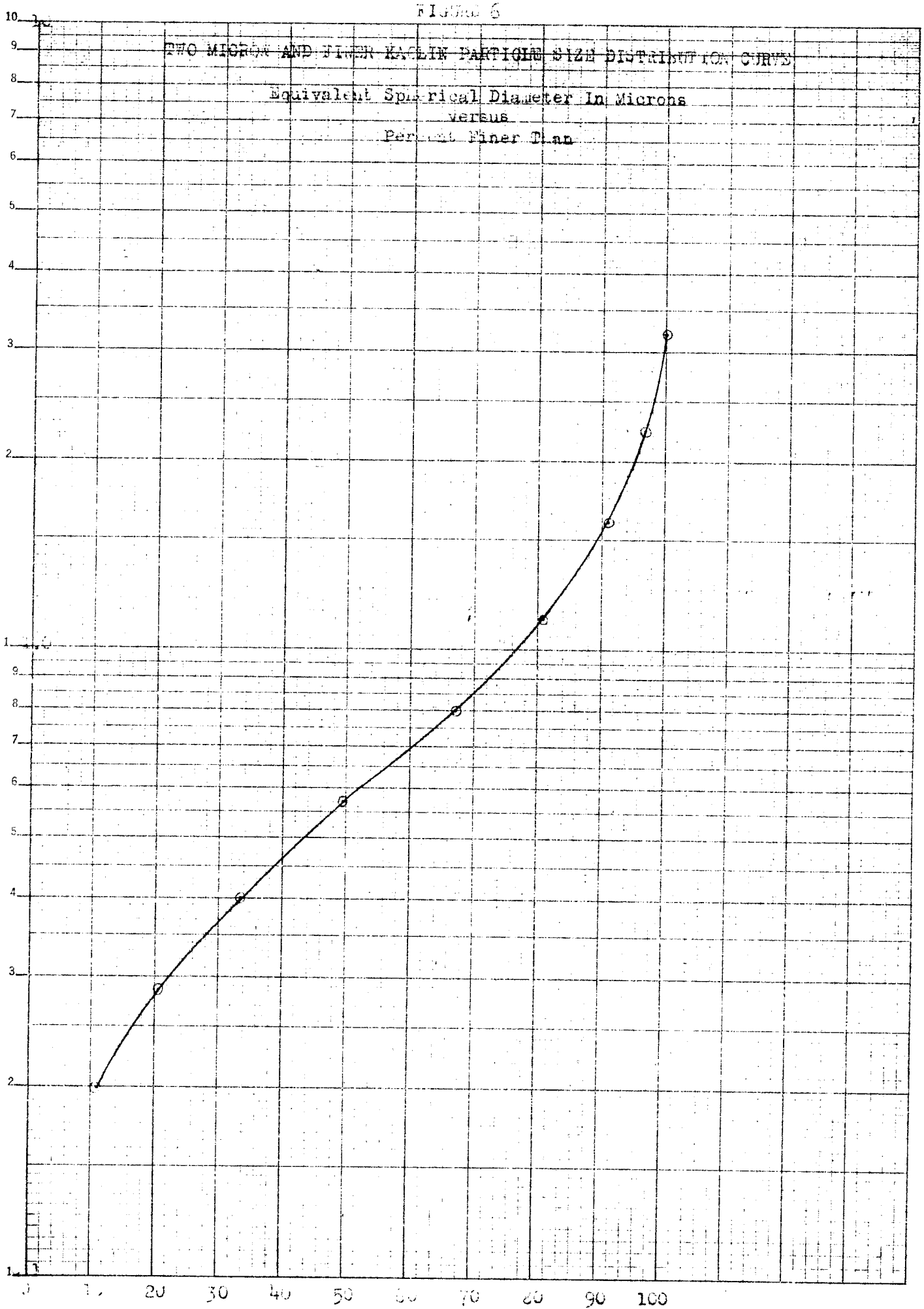

KEUFFEL & ESSER CO. MADE IN U.S.A.
2 CYCLES X 70 DIVISIONS

Experimental Results

Table II is a tabulation of the experimental results calculated from the original data presented in Table I.

The heat balance for 40 of the 51 runs were within 5%. The remaining 11 runs were within 10%. An analysis of the heat balances showed that the amount of heat transferred based on the condensate rate and steam quality are more accurate and more consistent than those based on the temperature rise of the slurry. Therefore, the heat transfer coefficients were based on the heat given up by the steam and not on the temperature rise of the slurry. (See Discussion of Results)

The six thermocouples, cemented into the brass pipe of the heat exchanger, indicated that the pipe wall temperature was no more than 5° F. below the temperature of the steam at the higher slurry flow rates. At the lower flow rates, the pipe temperature was close to the steam temperature.

Table III is a tabulation of the slurry viscosities at corresponding shear rates calculated from the original Fann viscometer data presented on Table I. Figures 7 through 14 are plots of the data from Table III. The curve or curves on each graph are for only one percentage concentration of solids. In most cases, one viscosity curve is used for more than one heat transfer run. A small variation in average bulk temperature had very little effect on the viscosity and, therefore, can be represented by one curve. More than one curve on a graph is due to a larger variation in average bulk temperature. These curves show the non-Newtonian behavior of the slurries. A Newtonian fluid would be represented by a horizontal line.

The bulk viscosity of the slurries flowing through the heat exchanger were determined by calculating the shear rate and finding the corresponding viscosity from the viscosity curves. The shear rate was calculated from the following equation (11):

$$\gamma = \frac{8V_b}{D}$$ Equation (12)

The viscosity determined by this method was used to correlate the heat transfer data.

The Reynolds numbers ranged from 0.9 to 2020 for the 51 runs.

The thermal conductivity of the slurries were calculated using the following equation (22):

$$K_b = K_1 \left[\frac{2K_1 + K_p - 2\,Xv\,(K_1 - K_p)}{2K_1 + K_p + Xv\,(K_1 - K_p)} \right]$$ Equation (11)

Where: Xv = fraction of solids by volume

K_b = thermal conductivity of slurry

K_1 = thermal conductivity of liquid

K_p = thermal conductivity of solids

The thermal conductivity of the slurries did not vary to any great extent with change in solids content and were within 10% of the value for water.

The effect of natural convection on the heat transfer coefficients was investigated by using the following equation (7):

$$\frac{hD}{k} = 1.75\,F_1 \left[\frac{wC}{kL} + 0.0722\left(\frac{D}{L} \right)^{0.75} N_{Gr}\,N_{Pr}\,F_2 \right]^{1/3}$$ Equation (10)

Where: F_1 and F_2 are dimensionless factors that can vary between 0 and 1.

N_{Gr} is the Grashof number - $\left(\frac{D^3\rho^2 g}{\mu^2}\right)(\beta\Delta T)$

N_{Pr} is the Prandtl number - $\left(\frac{C\mu}{k}\right)$

The empirical equation (8)

$$\frac{hD}{k} = 1.75 \left(\frac{wC}{kL}\right)^{1/3}$$ Equation (5)

is a standard equation that is used to calculate heat transfer coefficients in the laminar region. The additional term in equation (10), not included in equation (5), represents the correction for natural convection. Using equation (10), the correction for natural convection for 33 runs was less than 1%, for 11 runs it was less than 2% and for the remaining 7 runs it was less than 5%. The effect of natural convection was within experimental error and, therefore, could be disregarded.

Equations (5) and (10) were not used to correlate the heat transfer data because it was desired to use an equation having the Reynolds number as one of the dimensionless groups. Correlating the data with this type of equation would make it possible to put the Reynolds number on the abscissa of the graph which would easily show the range of the laminar region in which the work was done.

The following equation was used to correlate the heat transfer data:

$$\left(\frac{h_f}{C_b V_b \rho_b}\right)\left(\frac{C_b \mu_b}{K_b}\right)^{2/3} = d\left(\frac{DV_b \rho_b}{\mu_b}\right)^e$$ Equation (13)

Where: d and e are constants determined from the plot of the data.

Figure 15 is a plot of the heat transfer data for all 51 runs. From this plot, constants d and e were found to be 0.70 and - 2/3 respectively. The final heat transfer equation developed from this work is as follows:

$$\left(\frac{h_f}{C_b V_b \rho_b}\right)\left(\frac{C_b \mu_b}{K_b}\right)^{2/3} = 0.70 \left(\frac{D V_b \rho_b}{\mu_b}\right)^{-2/3} \qquad \text{Equation (14)}$$

for an $\frac{L}{D}$ ratio of 68.7.

TABLE II

TABULATION OF EXPERIMENTAL RESULTS

	Run No. 1	Run No. 2	Run No. 3	Run No. 4	Run No. 5	Run No. 6	Run No. 7	Run No. 8	Run No. 9	Run No. 10	Run No. 11	Run No. 12	Run No. 13	Run No. 14	Run No. 15	Run No. 16	Run No. 17	Run No. 18	Run No. 19	Run No. 2
w = lb/hr	1365	1110	863	600	426	135	199	1480	1280	976	739	443	104	150	1500	1230	840	495	118	266
t_o = °F	97.6	97.6	101.0	105.8	112.0	141.4	123.0	88.5	94.5	101.9	107.5	116.0	172.0	148.8	88.1	102.8	112.2	121.4	178.8	144.4
t_i = °F	83.4	84.0	82.3	82.8	82.8	82.8	81.5	73.5	80.4	83.4	83.4	84.0	84.0	83.4	71.0	82.3	85.7	86.6	86.6	85.4
$(t_o - t_i)$ = °F	14.2	13.6	18.7	23.0	29.2	58.6	41.5	15.0	14.1	18.5	24.1	32.0	88.0	65.4	18.1	20.5	26.5	34.8	92.2	58.6
X = % Solids	12.9	12.9	12.9	12.9	12.9	12.9	12.9	9.6	9.6	9.6	9.6	9.6	9.6	9.6	5.6	5.6	5.6	5.6	5.6	5.6
C_b = BTU/lb - °F	0.900	0.900	0.900	0.900	0.900	0.900	0.900	0.925	0.925	0.925	0.925	0.925	0.925	0.925	0.950	0.950	0.950	0.950	0.950	0.950
q_b = BTU/hr	17,440	13,600	14,500	12,450	11,200	7,120	7,430	20,500	16,700	16,600	16,480	13,100	8,460	10,580	25,800	24,000	21,200	16,400	10,300	14,700
w_c = lb/hr	17.50	15.50	14.40	13.60	12.91	7.57	8.80	21.00	19.21	17.80	16.20	13.79	9.20	10.90	27.40	24.95	22.60	17.39	10.80	15.50
H_s = BTU/lb	1138	1136	1137	1137	1137	1135	1133	1134	1134	1134	1134	1134	1134	1134	1134	1134	1134	1133	1134	1133
H_c = BTU/lb	214	210	212	214	214	200	200	206	207	206	208	202	204	203	206	207	207	202	208	200
ΔH = BTU/lb	924	926	925	923	923	935	933	928	927	928	926	932	930	931	928	927	927	931	926	933
q_s = BTU/hr	16,180	14,350	13,250	12,550	11,900	7,080	8,200	19,400	17,800	16,500	15,000	12,850	8,550	10,150	25,400	23,150	20,950	16,200	10,000	14,550
Δt_m = °F	156.5	151.2	154.0	153.8	149.1	118.1	131.0	159.0	147.5	148.8	146.8	136.1	104.9	116.8	159.4	147.7	140.1	130.1	102.3	115.1
h_f = BTU/hr-ft^2-°F	62.80	57.60	52.30	49.60	48.50	36.35	38.00	74.10	73.35	67.40	62.50	57.30	50.10	52.80	96.90	95.25	90.80	75.55	59.25	76.5
ρ_b = lb/ft^3	67.4	67.4	67.4	67.4	67.4	67.0	67.2	66.1	66.0	66.0	66.0	65.9	65.5	65.6	64.2	64.2	64.1	64.1	63.6	64.0
V_b = ft/sec	0.937	0.763	0.591	0.443	0.293	0.093	0.137	1.034	0.900	0.683	0.515	0.312	0.075	0.105	1.080	0.887	0.606	0.357	0.085	0.192
μ_b = lb/sec-ft	0.0895	0.1060	0.1300	0.1800	0.2320	0.5950	0.4450	0.0382	0.0405	0.0508	0.0655	0.1040	0.3650	0.2600	0.0109	0.0127	0.0168	0.0252	0.0785	0.0416
N_{Re}	61.6	42.3	26.8	13.5	7.4	0.9	1.8	156.4	128.0	77.5	45.3	17.3	1.2	2.3	555.5	392.0	202.5	79.3	6.0	25.8
K_b = BTU/hr-ft^2°F/ft	0.344	0.344	0.344	0.345	0.344	0.351	0.348	0.346	0.348	0.349	0.350	0.351	0.358	0.356	0.351	0.354	0.356	0.357	0.366	0.363
$N_{Pr} = \frac{C_b \mu_b}{K_b}$	842	998	1,225	1,691	2,185	4,490	4,145	368	388	485	623	988	3,375	2,435	106	123	161	242	734	394
$N_{Pr}^{2/3}$	88.5	99.9	114.5	141.5	167.0	310.0	258.0	51.2	53.0	61.5	72.5	99.0	224.0	181.0	22.4	24.7	29.6	38.9	81.0	57.5
$N_{st} \times 10^4 = \frac{h_f}{C_b V_b \rho_b}$	3.07	3.45	4.05	5.50	7.49	17.90	12.70	3.27	3.71	4.50	5.53	8.37	30.45	22.90	4.09	4.90	6.82	9.65	31.80	18.20
$\frac{N_{st} N_{Pr}^{2/3}}{\times 10^2}$	2,715	3,445	4,640	7.78	12.50	55.50	32.80	1.675	1.966	2.770	4.01	8.28	68.20	41.4	0.915	1.210	2.020	3.76	25.8	10.45

16	Run No. 17	Run No. 18	Run No. 19	Run No. 20	Run No. 21	Run No. 22	Run No. 23	Run No. 24	Run No. 25	Run No. 26	Run No. 27	Run No. 28	Run No. 29	Run No. 30	Run No. 31
0	840	495	118	266	1590	997	870	289	180	1380	364	300	832	1127	577
8	112.2	121.4	178.8	144.0	95.5	113.0	121.3	164.1	192.1	113.9	125.6	141.5	115.7	111.5	120.2
3	85.7	86.6	86.6	85.9	73.8	80.8	84.0	87.3	87.2	95.8	94.4	92.0	90.6	91.2	90.6
5	26.5	34.8	92.2	58.1	21.7	32.2	37.3	76.8	104.9	18.1	31.2	49.5	25.1	20.3	29.6
6	5.6	5.6	5.6	5.6	3.0	3.0	3.0	3.0	3.0	23.1	23.1	23.1	23.1	23.1	23.1
0	0.950	0.950	0.950	0.950	0.977	0.977	0.977	0.977	0.977	0.825	0.825	0.825	0.825	0.825	0.825
00	21,200	16,400	10,300	14,700	33,700	31,300	31,700	21,500	17,800	20,600	9,370	12,250	17,260	18,890	14,100
95	22.60	17.39	10.80	15.59	35.45	32.90	32.10	23.60	20.50	22.80	14.05	12.95	17.79	19.90	15.09
4	1134	1133	1134	1133	1134	1134	1134	1134	1134	1126	1126	1126	1126	1126	1126
7	207	202	208	200	207	208	208	206	208	211	209	207	206	200	199
7	927	931	926	933	927	926	926	928	926	915	917	919	920	926	927
50	20,950	16,200	10,000	14,550	32,850	30,400	29,700	21,900	18,950	20,000	12,890	12,900	16,350	18,100	14,000
.7	140.1	130.1	102.3	115.7	153.1	141.7	135.3	109.0	92.7	134.1	132.0	125.7	132.0	132.0	127.1
25	90.80	75.55	59.25	76.50	130.2	130.2	133.2	122.1	124.1	94.20	59.30	57.60	75.30	84.70	67.00
2	64.1	64.1	63.6	64.0	63.4	63.0	63.0	62.7	62.5	72.2	72.2	72.0	72.2	72.2	72.2
87	0.606	0.357	0.085	0.192	1.169	0.734	0.638	0.213	0.133	0.886	0.233	0.193	0.534	0.722	0.370
27	0.0168	0.0252	0.0785	0.0116	0.0032	0.0060	0.0063	0.0079	0.0102	0.1030	0.3040	0.3500	0.1580	0.1210	0.2100
2.0	202.5	79.3	6.0	25.8	2020.0	1010.0	616.0	147.9	71.7	54.3	4.8	3.5	21.3	37.7	11.1
54	0.356	0.357	0.366	0.361	0.356	0.359	0.360	0.367	0.371	0.333	0.335	0.336	0.333	0.332	0.332
23	161	242	734	394	31.6	39.1	42.0	75.6	96.7	919	2,695	3,090	1,110	1,082	1,879
4.7	29.6	38.9	81.0	57.5	10.0	11.55	12.07	17.8	21.0	94.3	193.0	211.5	125.0	105.0	151.5
.90	6.82	9.65	31.80	18.20	5.04	8.03	9.44	25.90	42.20	4.95	11.88	13.91	6.57	5.47	8.45
.210	2.020	3.76	25.8	10.15	0.504	0.928	1.139	4.61	8.86	4.67	22.93	29.60	8.21	5.75	12.80

Run No. 32	Run No. 33	Run No. 34	Run No. 35	Run No. 36	Run No. 37	Run No. 38	Run No. 39	Run No. 40	Run No.
1462	990	750	570	315	1440	1185	1470	1005	1
116.6	120.7	120.2	124.1	134.7	112.0	115.7	112.1	122.0	1
98.6	98.6	97.4	95.7	94.6	94.7	96.6	92.1	95.9	1
18.0	22.1	22.8	28.4	40.1	17.3	19.1	20.0	26.1	
20.4	20.4	20.4	20.4	20.4	20.4	20.4	13.7	13.7	
0.843	0.843	0.843	0.843	0.843	0.843	0.843	0.896	0.896	0
21,600	18,450	14,400	13,650	10,680	21,000	19,100	26,400	23,550	2
22.60	18.07	16.20	14.67	12.10	21.40	19.75	27.65	24.50	2
1126	1125	1125	1126	1126	1125	1125	1128	1121	1
204	202	201	204	205	198	200	208	204	
922	923	924	922	921	927	925	920	917	
20,850	16,670	14,980	13,520	11,140	19,850	18,250	25,450	22,500	2
128.1	123.1	123.8	125.2	121.8	129.0	126.2	136.8	124.7	
99.00	82.25	73.50	65.70	55.60	93.50	88.00	117.1	109.4	
70.6	70.6	70.6	70.6	70.5	70.7	70.7	67.9	67.7	
0.936	0.649	0.492	0.374	0.207	0.942	0.777	1.001	0.687	
0.710	0.0885	0.1110	0.1400	0.2270	0.0665	0.0770	0.0202	0.0278	
81.3	45.3	27.4	16.5	5.6	87.5	62.8	296.1	146.4	2
0.338	0.338	0.338	0.338	0.340	0.337	0.337	0.346	0.348	
637	795	995	1,258	2,030	599	694	188	258	
73.7	85.7	99.8	116.5	160.5	71.0	78.3	32.8	40.4	
4.93	5.91	6.95	8.20	12.52	4.60	5.28	5.32	7.30	
3.63	5.06	6.94	9.55	20.10	3.27	4.14	1.746	2.95	

Run No. 30	Run No. 31	Run No. 32	Run No. 33	Run No. 34	Run No. 35	Run No. 36	Run No. 37	Run No. 38	Run No. 39	Run No. 40	Run No. 41	Run No. 42	Run No. 43	Run No. 44	Run No. 45	Run No. 46	Run No. 47	Run No. 48	Run No. 49	Run No. 50	Run No. 51
1127	577	1462	990	750	570	315	1440	1185	1470	1005	1230	540	385	802	1500	1200	840	720	1365	840	1455
111.5	120.2	116.6	120.7	120.2	124.1	134.7	112.0	115.7	112.1	122.0	125.1	147.1	152.7	126.4	108.3	115.2	121.5	127.2	112.0	122.7	110.2
91.2	90.6	98.6	98.6	97.4	95.7	94.6	94.7	96.6	92.1	95.9	103.0	104.2	103.5	100.0	87.8	91.6	94.1	96.6	94.5	94.1	92.6
20.3	29.6	18.0	22.1	22.8	28.4	40.1	17.3	19.1	20.0	26.1	22.1	42.9	49.2	26.4	20.5	23.6	27.4	30.6	17.5	28.6	17.6
23.1	23.1	20.4	20.4	20.4	20.4	20.4	20.4	20.4	13.7	13.7	13.7	13.7	13.7	13.7	10.1	10.1	10.1	10.1	10.1	10.1	10.1
0.825	0.825	0.843	0.843	0.843	0.843	0.843	0.843	0.843	0.896	0.896	0.896	0.896	0.896	0.896	0.923	0.923	0.923	0.923	0.923	0.923	0.923
18,890	14,100	21,600	18,450	14,400	13,650	10,680	21,000	19,100	26,400	23,550	24,400	20,750	16,930	18,970	28,400	26,100	21,250	20,350	22,100	22,200	23,650
19.90	15.09	22.60	18.07	16.20	14.67	12.10	21.40	19.75	27.65	24.50	26.90	21.95	17.85	19.80	29.50	29.80	23.45	22.60	24.70	23.35	24.70
1126	1126	1126	1125	1125	1126	1126	1125	1125	1128	1121	1122	1122	1122	1121	1121	1127	1128	1122	1121	1122	1122
200	199	204	202	201	204	205	198	200	208	204	204	209	209	198	203	204	207	205	201	203	202
926	927	922	923	924	922	921	927	925	920	917	918	913	913	923	918	923	921	917	920	919	920
18,400	14,000	20,850	16,670	14,980	13,520	11,140	19,850	18,250	25,450	22,500	24,700	20,050	16,300	18,300	27,100	27,500	21,600	20,700	22,700	21,450	22,700
132.0	127.1	128.1	123.1	123.8	125.2	121.8	129.0	126.2	136.8	124.7	119.8	115.2	112.4	115.1	133.8	132.0	127.0	122.4	126.7	126.0	130.6
84.70	67.00	99.00	82.25	73.50	65.70	55.60	93.50	88.00	117.1	109.4	125.2	105.8	88.1	100.2	123.0	120.0	103.2	102.7	108.8	103.5	110.0
72.2	72.2	70.6	70.6	70.6	70.6	70.5	70.7	70.7	67.9	67.7	67.5	67.4	67.4	67.5	65.7	65.8	66.0	66.0	66.0	66.0	66.0
0.722	0.370	0.936	0.649	0.492	0.374	0.207	0.942	0.777	1.001	0.687	0.845	0.372	0.265	0.551	1.0555	0.842	0.590	0.505	0.958	0.590	1.020
0.1210	0.2100	0.710	0.0885	0.1110	0.1400	0.2270	0.0665	0.0770	0.0202	0.0278	0.0225	0.0440	0.0600	0.0331	0.0097	0.0114	0.0146	0.0158	0.0104	0.0146	0.0099
37.7	11.1	81.3	45.3	27.4	16.5	5.6	87.5	62.8	296.1	146.4	221.0	49.9	26.0	98.2	625.0	424.0	233.0	184.0	532.0	233.0	594.0
0.332	0.332	0.338	0.338	0.336	0.338	0.340	0.337	0.337	0.346	0.348	0.349	0.353	0.353	0.349	0.350	0.351	0.853	0.354	0.351	0.353	0.350
1,082	1,879	637	795	995	1,258	2,030	599	694	188	258	208	402	549	306	92.1	108.1	137.5	148.3	90.6	137.5	94.0
105.0	151.5	73.7	85.7	99.8	116.5	160.5	71.0	78.3	32.8	40.4	35.1	54.7	67.0	45.3	20.4	22.6	26.6	28.0	21.4	26.6	20.6
5.47	8.45	4.93	5.91	6.95	8.20	12.52	4.60	5.28	5.32	7.30	6.78	13.02	15.22	8.32	5.30	6.48	7.96	9.25	5.16	7.98	4.90
5.75	12.80	3.63	5.06	6.94	9.55	20.10	3.27	4.14	1.746	2.95	2.38	7.12	10.20	3.77	1.08	1.465	2.12	2.59	1.105	2.12	1.216

TABLE III

TABULATION OF SLURRY VISCOSITY VERSUS SHEAR RATE

RPM	600		300		200		100		6		3	
Shear Rate (Sec -1)	942		471		314		157		9.42		4.71	
	Scale Rdg	Visc x_3 10^3	Scale Rdg	Visc x_3 10^3	Scale Rdg	Visc x_3 10^3	Scale Rdg	Visc x_3 10^3	Scale Rdg	Visc x_3 10^3	Scale Rdg	Visc x_3 10^3
Run No.	LB/FT^2	LB FT.SEC	LB/FT^2	LB FT.SEC	LB/FT^2	LB FT.SEC	LB/FT^2	LB FT.SEC	LB/FT^2	LB FT.SEC	LB/FT^2	LB FT.SEC
1	0.365	12.5	0.315	21.5	0.298	30.6	0.267	54.8	0.170	581.0	0.135	922.0
2	0.365	12.5	0.315	21.5	0.298	30.6	0.267	54.8	0.170	581.0	0.135	922.0
3	0.365	12.5	0.315	21.5	0.298	30.6	0.267	54.8	0.170	581.0	0.135	922.0
4	0.362	12.4	0.315	21.5	0.300	30.8	0.275	56.4	0.172	587.0	0.132	902.0
5	0.365	12.5	0.315	21.5	0.298	30.6	0.267	54.8	0.170	581.0	0.135	922.0
6	0.352	12.1	0.305	20.8	0.305	31.3	0.272	55.8	0.165	564.0	0.125	855.0
7	0.360	12.3	0.315	21.5	0.315	32.3	0.276	56.6	0.180	615.0	0.135	922.0
8	0.198	6.8	0.162	11.1	0.137	14.0	0.118	24.2	0.085	290.0	0.075	512.0
9	0.185	6.3	0.147	10.1	0.132	13.5	0.115	23.6	0.075	256.0	0.067	458.0
10	0.185	6.3	0.147	10.1	0.132	13.5	0.115	23.6	0.075	256.0	0.067	458.0
11	0.185	6.3	0.147	10.1	0.132	13.5	0.115	23.6	0.075	256.0	0.067	458.0
12	0.175	6.0	0.145	9.9	0.132	13.5	0.115	23.6	0,080	273.0	0.070	479.0
13	0.165	5.6	0.135	9.2	0.125	12.8	0.115	23.6	0.085	290.0	0.072	492.0
14	0.165	5.6	0.132	9.0	0.128	13.1	0.112	23.0	0.080	273.0	0.068	465.0
15	0.080	2.7	0.055	3.8	0.050	5.1	0.035	7.2	0.020	68.4	0.015	103.0
16	0.075	2.6	0.055	3.8	0.048	4.9	0.035	7.2	0.022	75.1	0.020	137.0
17	0.072	2.5	0.055	3.8	0.047	4.8	0.035	7.2	0.020	68.4	0.020	137.0
18	0.072	2.5	0.055	3.8	0.047	4.8	0.035	7.2	0.020	68.4	0.020	137.0
19	0.060	2.0	0.048	3.3	0.042	4.3	0.035	7.2	0.022	75.1	0.015	103.0
20	0.065	2.2	0.050	3.4	0.045	4.6	0.035	7.2	0.022	75.1	0.018	123.0
21	0.038	1.3	0.025	1.7	0.020	2.0	0.013	2.7	0.005	17.1	0.002	13.7

TABLE III (cont.)

TABULATION OF SLURRY VISCOSITY VERSUS SHEAR RATE

RPM	600		300		200		100		6		3	
Shear Rate (Sec -1)	942		471		314		157		9.42		4.71	
	Scale Rdg	Visc x 10^3	Scale Rdg	Visc x 10^3	Scale Rdg	Visc x 10^3	Scale Rdg	Visc x 10^3	Scale Rdg	Visc x 10^3	Scale Rdg	Visc x 10^3
Run No.	LB/FT^2	LB/FT.SEC	LB/FT^2	LB/FT.SEC	LB/FT^2	LB/FT.SEC	LB/FT^2	LB/FT.SEC	LB/FT^2	LB/FT.SEC	LB/FT^2	LB/FT.SEC
22	0.035	1.2	0.022	1.5	0.017	1.7	0.012	2.5	0.005	17.1	0.002	13.7
23	0.035	1.2	0.022	1.5	0.017	1.7	0.012	2.5	0.005	17.1	0.002	13.7
24	0.030	1.0	0.020	1.4	0.017	1.7	0.012	2.5	0.005	17.1	0.002	13.7
25	0.030	1.0	0.020	1.4	0.017	1.7	0.012	2.5	0.005	17.1	0.002	13.7
26	0.419	14.3	0.369	25.2	0.340	34.8	0.301	61.7	0.177	604.0	0.135	922.0
27	0.419	14.3	0.369	25.2	0.340	34.8	0.301	61.7	0.177	604.0	0.135	922.0
28	0.402	13.7	0.355	24.3	0.330	33.8	0.290	59.5	0.175	598.0	0.090	615.0
29	0.410	14.0	0.362	24.8	0.335	34.3	0.300	61.5	0.180	615.0	0.130	889.0
30	0.419	14.3	0.369	25.2	0.340	34.8	0.301	61.7	0.177	604.0	0.135	922.0
31	0.419	14.3	0.369	25.2	0.340	34.8	0.301	61.7	0.177	604.0	0.135	922.0
32	0.280	9.6	0.241	17.9	0.221	22.7	0.194	39.8	0.120	410.0	0.100	684.0
33	0.280	9.6	0.241	17.9	0.221	22.7	0.194	39.8	0.120	410.0	0.100	684.0
34	0.280	9.6	0.241	17.9	0.221	22.7	0.194	39.8	0.120	410.0	0.100	684.0
35	0.280	9.6	0.241	17.9	0.221	22.7	0.194	39.8	0.120	410.0	0.100	684.0
36	0.275	9.4	0.235	16.1	0.220	22.6	0.192	39.4	0.120	410.0	0.100	684.0
37	0.287	9.8	0.245	16.8	0.223	22.9	0.200	41.0	0.125	427.0	0.100	684.0
38	0.283	9.7	0.243	16.6	0.222	22.8	0.197	40.4	0.123	420.0	0.100	684.0
39	0.109	3.7	0.088	6.0	0.075	7.7	0.062	12.7	0.045	154.0	0.041	280.5
40	0.103	3.5	0.083	5.7	0.073	7.5	0.061	12.5	0.044	150.0	0.041	280.5
41	0.101	3.5	0.081	5.5	0.072	7.4	0.060	12.3	0.043	147.0	0.040	273.5
42	0.093	3.2	0.079	5.4	0.069	7.1	0.052	10.7	0.042	143.5	0.038	260.0

TABLE III (Cont.)

TABULATION OF SLURRY VISCOSITY VERSUS SHEAR RATE

RPM	600		300		200		100		6		3	
Shear Rate (Sec -1)	942		471		314		157		9.42		4.71	
	Scale Rdg	Visc x 10^3	Scale Rdg	Visc x 10^3	Scale Rdg	Visc x 10^3	Scale Rdg	Visc x 10^3	Scale Rdg	Visc x 10^3	Scale Rdg	Visc x 10^3
Run No.	$\frac{LB}{FT^2}$	$\frac{LB}{FT.SEC}$	$\frac{LB}{FT^2}$	$\frac{LB}{FT.SEC}$	$\frac{LB}{FT^2}$	$\frac{LB}{FT.SEC}$	$\frac{LB}{FT^2}$	$\frac{LB}{FT.SEC}$	$\frac{LB}{FT^2}$	$\frac{LB}{FT.SEC}$	$\frac{LB}{FT^2}$	$\frac{LB}{FT.SEC}$
43	0.093	3.2	0.079	5.4	0.069	7.1	0.052	10.7	0.042	143.5	0.038	260.0
44	0.101	3.5	0.081	5.5	0.072	7.4	0.060	12.3	0.043	147.0	0.040	273.5
45	0.068	2.3	0.049	3.4	0.041	4.2	0.031	6.4	0.018	61.5	0.013	89.0
46	0.063	2.1	0.047	3.2	0.041	4.2	0.031	6.4	0.017	58.1	0.013	89.0
47	0.061	2.1	0.047	3.2	0.041	4.2	0.031	6.4	0.016	54.7	0.012	82.1
48	0.059	2.0	0.043	2.9	0.039	4.0	0.030	6.2	0.015	51.3	0.012	82.1
49	0.063	2.1	0.047	3.2	0.041	4.2	0.031	6.4	0.017	58.1	0.013	89.0
50	0.061	2.1	0.046	3.1	0.041	4.2	0.031	6.4	0.016	54.7	0.012	82.1
51	0.068	2.3	0.049	3.4	0.041	4.2	0.031	6.4	0.018	61.5	0.013	89.0

FIGURE 7

VISCOSITY OF 12.9% HALF MICRON AND FINER KAOLIN SLURRY

Viscosity vs. Shear Rate

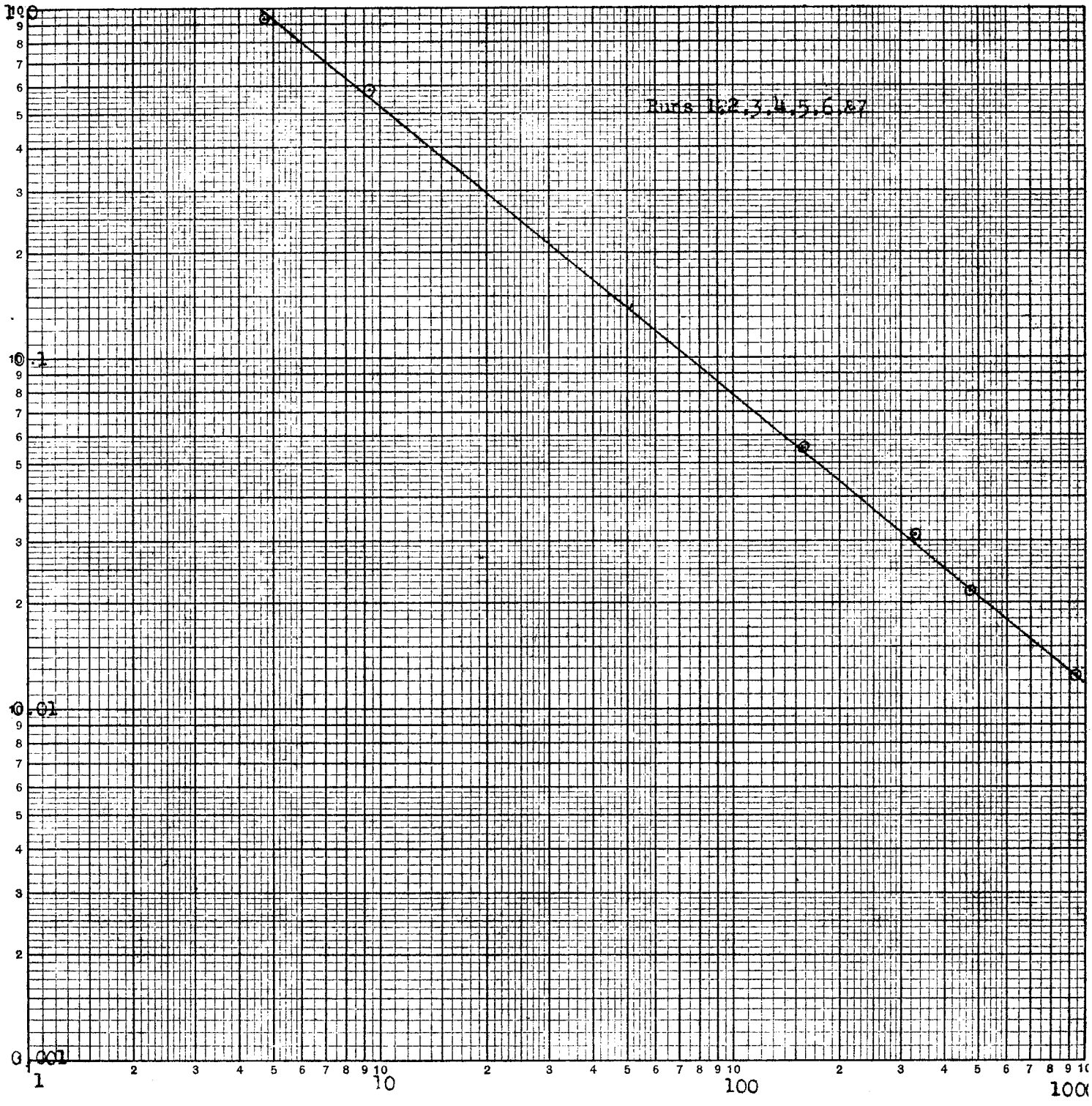

Shear Rate, $sec.^{-1}$

FIGURE 9

VISCOSITY OF 5.6% HALF MICRON AND FINER KAOLIN SLURRY

Viscosity vs. Shear Rate

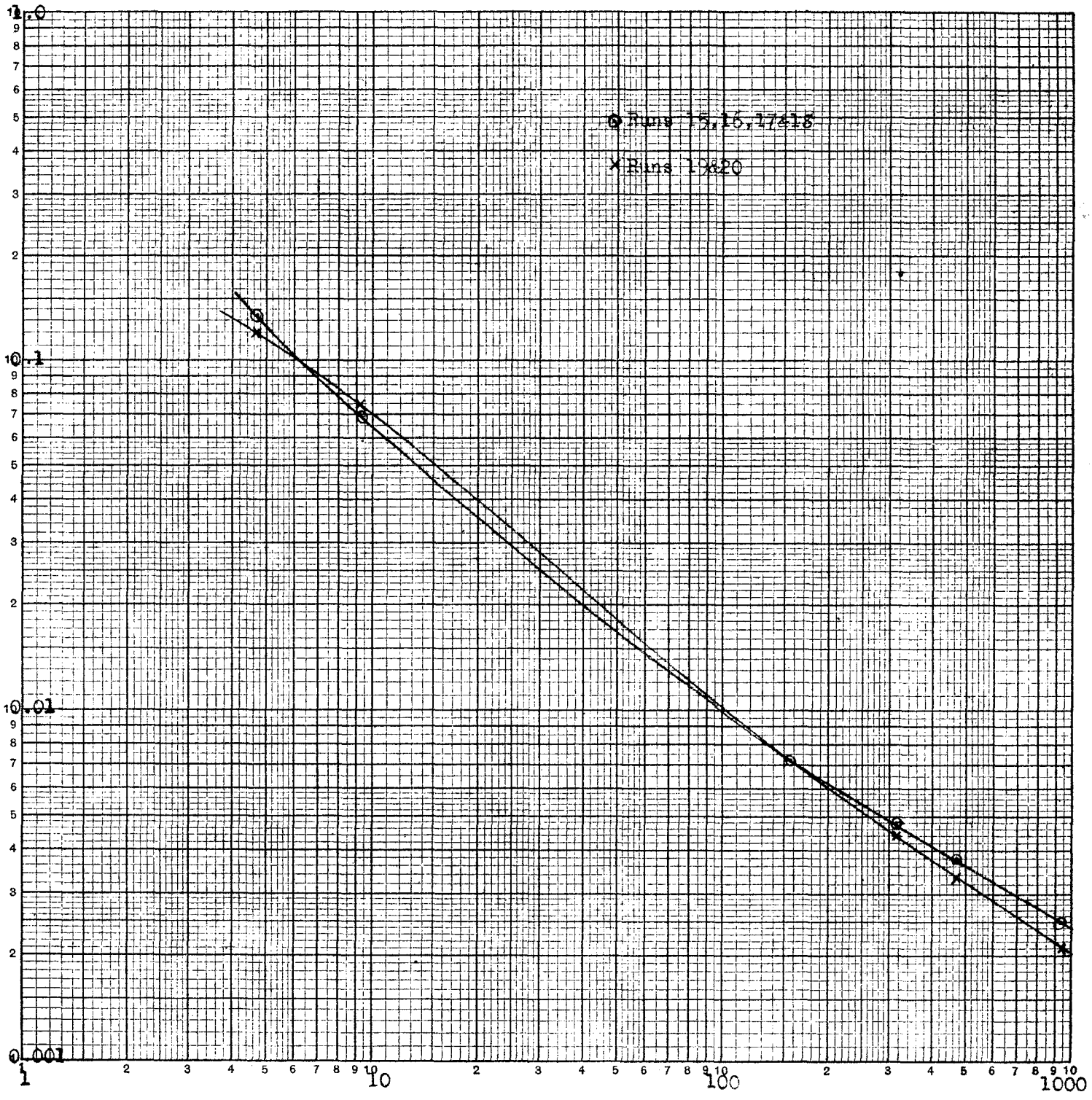

FIGURE 10

VISCOSITY OF 3.0% HALF MICRON AND FINER KAOLIN SLURRY

Viscosity vs. Shear Rate

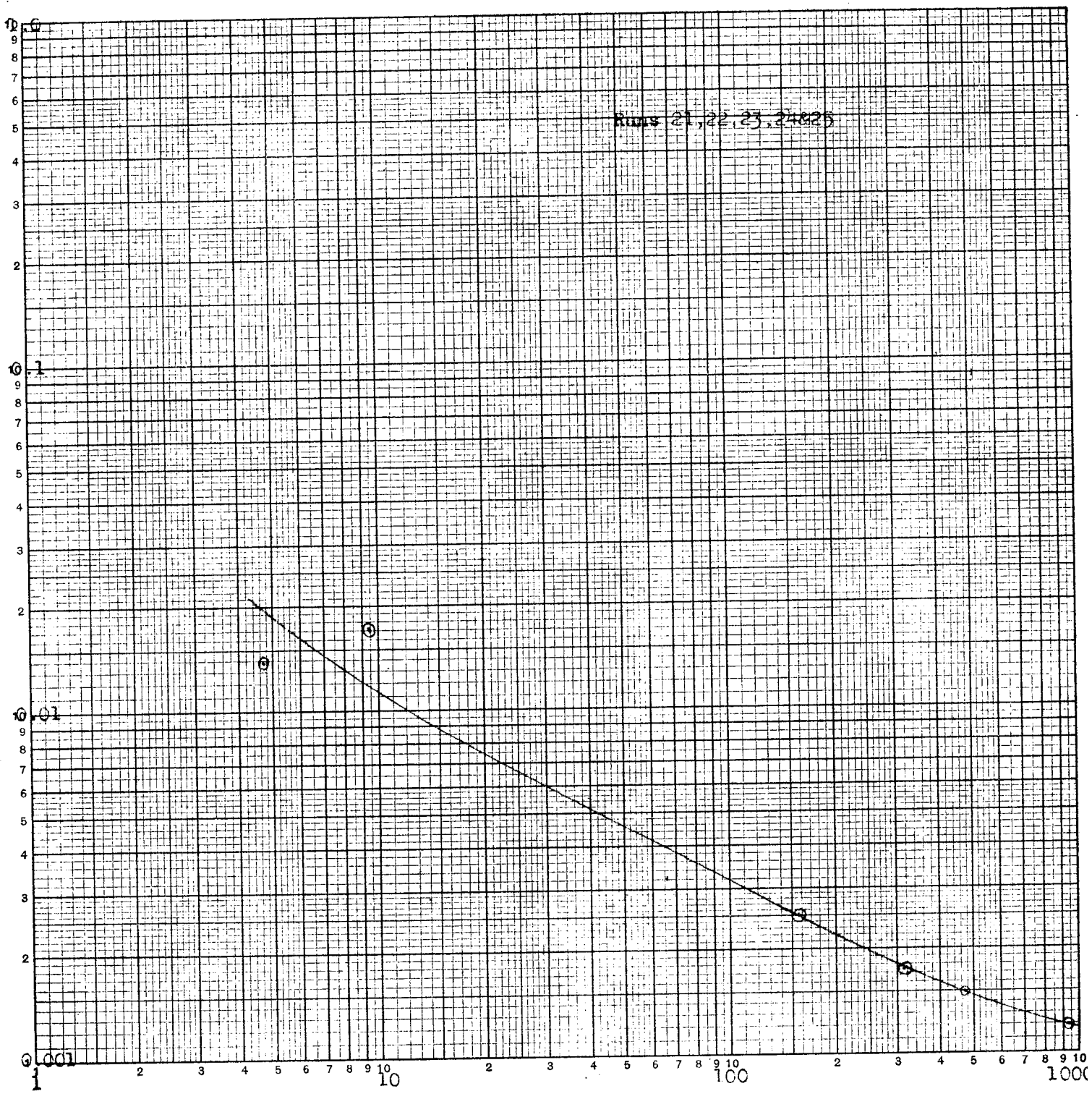

FIGURE 11

VISCOSITY OF 23.1% TWO MICRON AND FINER KAOLIN SLURRY

Viscosity vs. Shear Rate

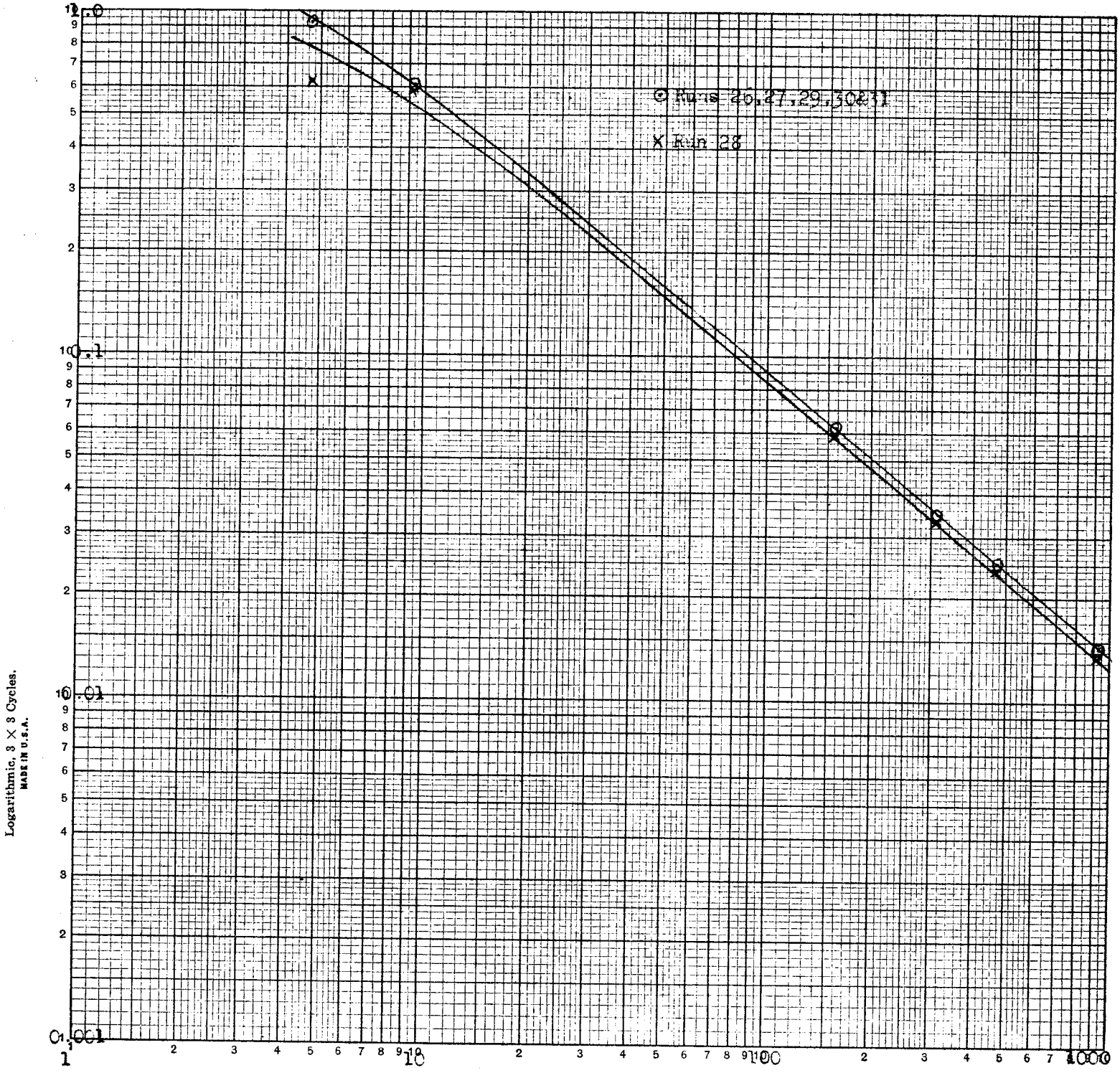

FIGURE 12

VISCOSITY OF 20.4% TWO MICRON AND FINER KAOLIN SLURRY

Viscosity vs. Shear Rate

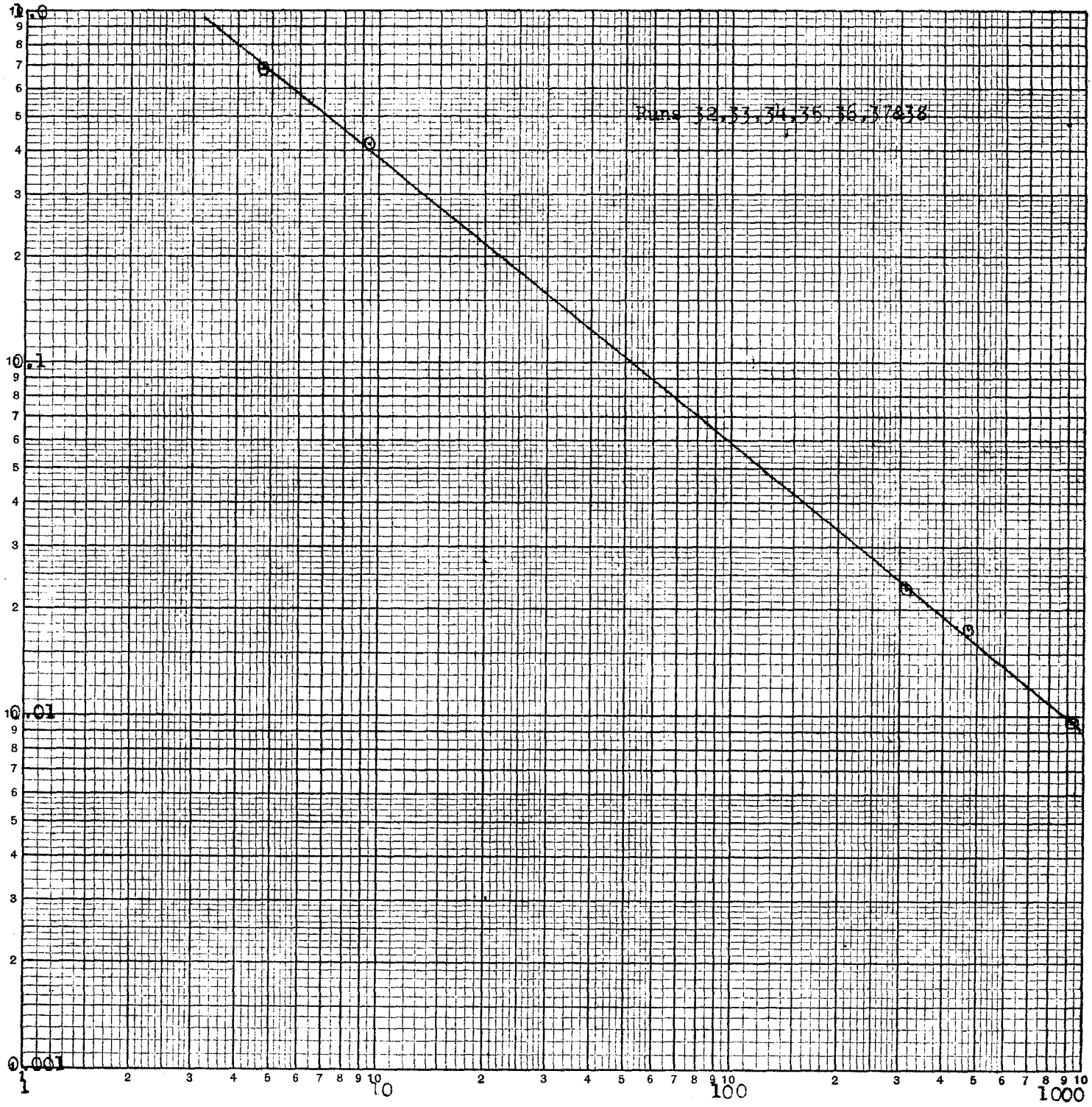

Logarithmic, 3 × 3 Cycles.
MADE IN U.S.A.

FIGURE 13

VISCOSITY OF 13.7% TWO MICRONS AND FINER KAOLIN SLURRY

Viscosity vs. Shear Rate

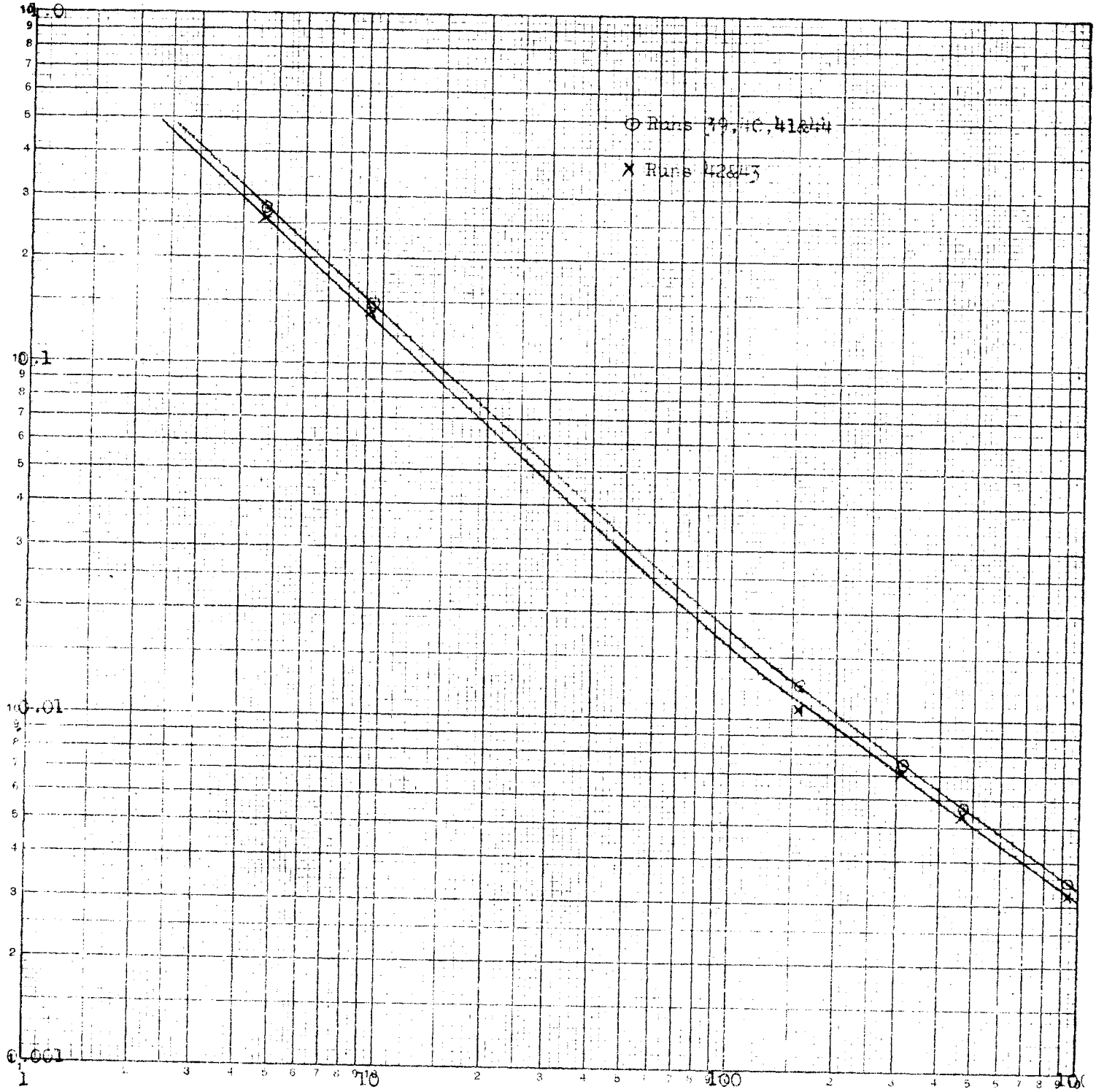

KEUFFEL & ESSER CO. MADE IN U.S.A.

FIGURE 14

VISCOSITY OF 10.1% TWO MICRON AND FINER KAOLIN SLURRY

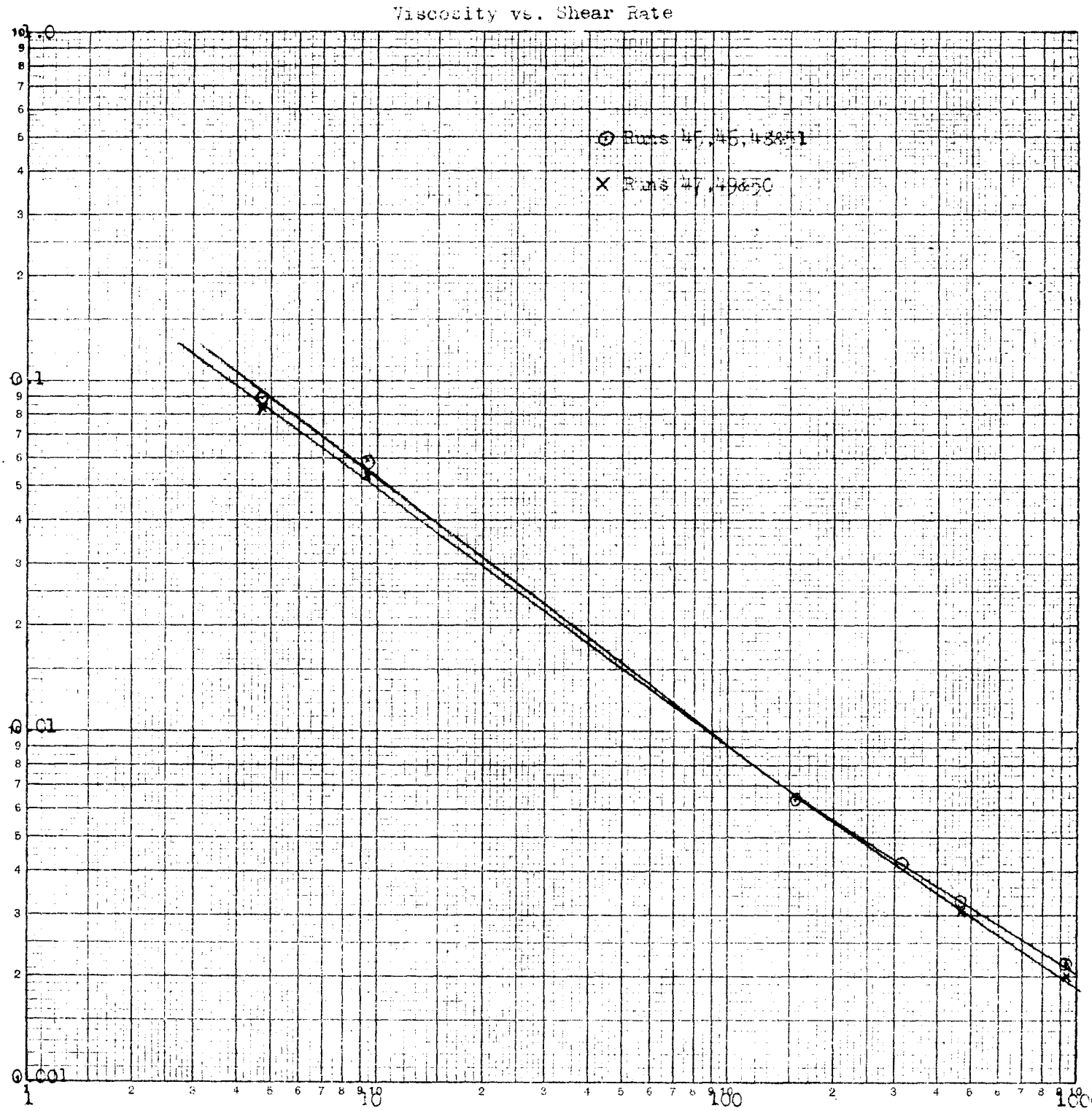

KEUFFEL & ESSER CO. MADE IN U.S.A.
359-120
X 3 CYCLES

CORRELATION OF HEAT TRANSFER DATA

FIGURE 15

$(St)(Pr)^{2/3}$ versus (Re)

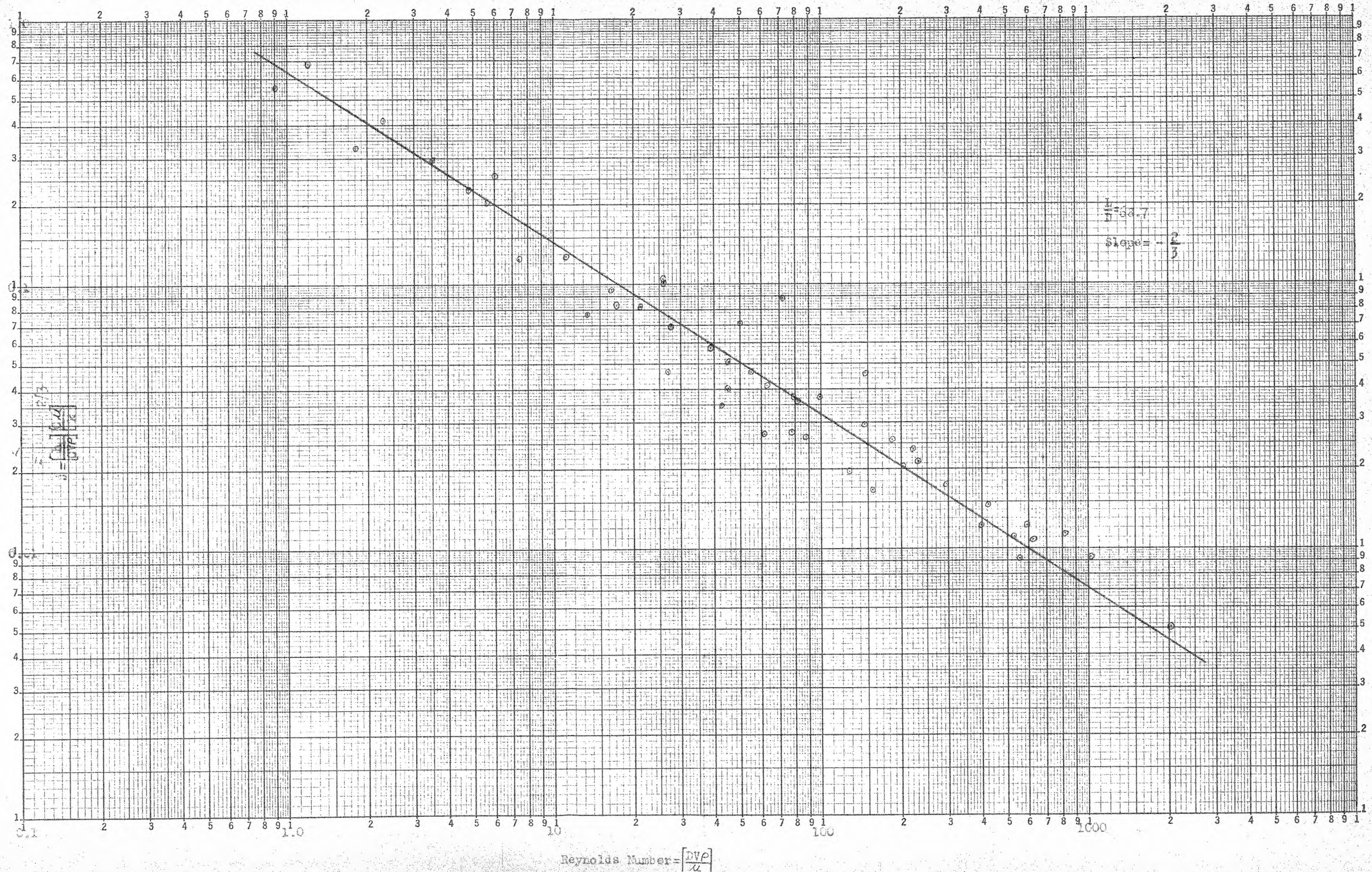

Discussion of Results

The heat balances were rather satisfactory. The heat transferred based on the steam quality and condensate rate was accurate to three significant figures. Based on the temperature rise of the slurry at the higher flow rates, it was also accurate to three figures, however, at the lower flow rates it was accurate to only two figures. This was due to a fluctuation in the outlet temperature which varied as much as 10% of the temperature rise of the slurry even though the temperature was taken after the slurry flowed through a mixing valve. Without any method of mixing, even at the higher flow rates, it was found that there was much error in the outlet temperature. Plotting the heat balances versus the flow rate showed that the data based on the heat content of the steam was more reliable. The plots of this data always formed a smooth curve, while the data based on the temperature rise of the slurry often straddled on both sides of this curve, especially at the lower flow rates. As a result, the heat transfer coefficients were based only on the heat given up by the steam and not on the temperature rise of the slurry. It should be pointed out that with a guard jacket on the heat exchanger and the entire unit well insulated, including the steam trap, the heat losses were quite small. Also, the steam calorimeter was located at the entrance of the heat exchanger steam jacket.

The first approach in determining the viscosity of the slurries was by means of a pipeline viscometer. The pressure drop due to friction, through a 1" x 9' long pipe was so small that it could not be measured to any degree of accuracy, especially at the lower flow rates. This method was, therefore, not used. A literature search was made to find

other methods of determining viscosity that could be used instead. A method used by many investigations was to use laboratory viscometer data and relate these data to pipeline flow.

A Fann viscometer was used to determine the viscosity of the slurries. This instrument, which is rather an expensive piece of laboratory equipment, was just reconditioned before it was used. This is one of the types of viscometers used in the clay industry to measure viscosities of clay slurries. The data from the Fann viscometer was significant to three figures. The viscosity curves, shown on Figures 7 through 14, are, no doubt, a rather accurate representation of the non-Newtonian behavior of the slurries. Using the equation $\dot{\gamma} = \frac{8V_b}{D}$, the shear rates of the slurries flowing through the heat exchanger were calculated using the average velocity. From the viscosity curves, which were determined at the average temperature the slurry was at in the heat exchanger, the shear rate was used to find the corresponding bulk viscosity. This viscosity was used to correlate the heat transfer data. A variation in the mass rate through the heat exchanger by a factor of ten caused the bulk viscosity to change by about a factor of thirty. Therefore, by increasing the mass rate by a factor of 10 caused the Reynolds number to increase by about a factor of 300, since the slurries were pseudoplastic. The non-Newtonian behaviors of the fluids used were not known at the time of the equipment design. This made sizing the equipment and establishing flow rates difficult.

Several additional comments can be made about the viscosity curves shown on Figures 7 through 14. Generally speaking, the slopes of all the

viscosity curves are approximately the same. However, as the solids content of the slurry became greater, there is a tendency for the viscosity curves to have a slightly greater slope, indicating a more non-Newtonian behavior. Also, an increase in solids caused the viscosity curves to shift upward on the graphs, indicating higher viscosity. At the same solids content, the finer kaolin produced a higher slurry viscosity than the coarser material, but the non-Newtonian behavior (i.e. slope of curve) was about the same for both materials.

The following equation (7) was used to determine the effect of a natural convection on the heat transfer coefficients:

$$\frac{hD}{K} = 1.75\, F_1 \left[\frac{wC}{KL} + 0.0722 \left(\frac{D}{L} N_{Gr}, N_{Pr} \right)^{0.75} F_2 \right]^{1/3}$$

Equation (10)

Where: F_1 and F_2 are dimensionless factors that can vary between 1 and 0.

N_{Gr} is the Grashof number $\left(\frac{D^3 \rho^2 g}{\mu^2} \right) (B\Delta t)$

N_{Pr} is the Prandtl number $\left(\frac{C\mu}{K} \right)$

This equation is for heating fluids flowing vertically upward. The Nusselt numbers varied from 9.07 to 32.35. The Grashof numbers varied from 0.188 to 6300. The Prandtl numbers varied from 31.6 to 5490.

The correction for natural convection was quite small for all 51 runs and within experimental error. The correction for natural convection was, therefore, disregarded. It was found, however, that at the higher flow rates along with higher viscosities, the correction for natural convection

was very small. Conversely, at the lower flow rates along with lower viscosity, the correction became more significant. However, it was still less than 5% of the Nusselt number.

It was brought out in the Experimental Results that it was desired to correlate the heat transfer data using an equation which had the Reynolds number as one of the dimensionless groups. This made it possible to plot the data with the Reynolds number on the abscissa of the graph easily showing in what range of the laminar region the work was done. The equation that was selected to correlate the data was of the same form as that developed by Sieder and Tate. This equation can be expressed in two different ways:

$$\left(\frac{h_f}{C_b V_b \rho_b}\right)\left(\frac{C_b \mu_b}{K_b}\right)^{2/3}\left(\frac{\mu_w}{\mu_b}\right)^{0.14}\left(\frac{L}{D}\right)^{1/3} = d\left(\frac{DV_b\rho_b}{\mu_b}\right)^{e}$$

Equation (13)

or

$$\left(\frac{h_f D}{K_f}\right)\left(\frac{C_b \mu_b}{K_b}\right)^{-1/3}\left(\frac{\mu_w}{\mu_b}\right)^{0.14}\left(\frac{L}{D}\right)^{1/3} = f\left(\frac{DV_b\rho_b}{\mu_b}\right)^{g}$$

Equation (13a)

Where: d, e, f, and g are constants determined from the plot of the data. As can be seen from Figure 15, the heat transfer data was correlated using Equation (13). The data gave a rather satisfactory plot and, therefore, it was felt that there was no need to develop a special equation based on this work.

The heat transfer equation resulting from this work is as follows:

$$\left(\frac{h_f}{C_b V_b \rho_b}\right)\left(\frac{C_b \mu_b}{K_b}\right)^{2/3} = 0.70\left(\frac{DV_b\rho_b}{\mu_b}\right)^{-2/3}$$

Equation (14)

This equation is for an L/D ratio of 68.7. The Sieder and Tate Equation (21) for laminar flow is as follows:

$$\left(\frac{h}{CV\rho}\right)\left(\frac{C\mu}{K}\right)^{2/3}\left(\frac{L}{D}\right)^{1/3}\left(\frac{\mu_w}{\mu_b}\right)^{0.14} = 1.86\left(\frac{DV\rho}{\mu}\right)^{-2/3}$$

Equation (15)

For an L/D of 68.7, this equation becomes:

$$\left(\frac{h}{CV\rho}\right)\left(\frac{C\mu}{K}\right)^{2/3}\left(\frac{\mu_w}{\mu_b}\right)^{0.14} = 0.455\left(\frac{DV\rho}{\mu}\right)^{-2/3}$$

Equation (16)

The Reynolds number exponent was found to be the same from this work as that of the Sieder and Tate equation. However, there is a difference in the intercepts. Substituting 68.7 in the Sieder and Tate equation for the L/D term, the constant becomes 0.455. From this work it was found to be 0.70. This difference, is no doubt, mostly due to the viscosity correction term included in the Sieder and Tate equation but not included in the equation developed from this work. The reason for not including this term was because there was no data available and to obtain the necessary data would have been quite a difficult task. Also, it was felt that this term would make only a small difference in the final correlation and, therefore, could be disregarded.

In order to get a constant of 0.455 in the equation resulting from this work, the $\left(\frac{\mu_w}{\mu_b}\right)^{0.14}$ term, if included in this equation, would have to be equal to 0.65. In the case of a Newtonian fluid, the viscosity term is usually less than one. For example, with an average bulk temperature of 100°F and a pipe wall temperature of 235°F, this viscosity term for water is equal to 0.839. At these two temperatures, which are in the

same range as the slurry temperatures, the viscosity of water changes by a factor of 3.5. However, the average change between the bulk viscosity and the wall viscosity of the slurries, calculated from $\frac{\mu_w}{\mu_b}^{0.14} = 0.65$ is found to be 21.8 times. The effect of temperature on the viscosity of the slurries is probably close to that for water. From what is known about the slurries, it is believed that the shear rate has more effect on the viscosity than the temperature. The difference between the values of 21.8, calculated for the slurries, and 3.5, which is probably close to the average value for the temperature effect on the viscosities of the slurries, is probably due to their non-Newtonian behavior.

The greatest shear rate must be close to the pipe wall and not in the center of the stream. Close to the wall, both the higher temperature and greater shear rate could cause the viscosity to decrease by this large (21.8 times) amount. This could account for a large difference between the bulk viscosity and the wall viscosity. In order to study this more thoroughly, more heat transfer and viscosity data are needed. The omission of this viscosity correction factor might possibly account for some of the spread of the data.

Several comments can be made about the effect of solids content and particle size on the heat transfer coefficients. The coefficients had a tendency to increase with increase in particle size and decrease with increase in solids content. These two variables were taken indirectly into account to some degree in the viscosity term when the heat transfer data was correlated.

CONCLUSIONS

An equation similar in form to the Sieder-Tate equation for Newtonian fluids can be used to calculate the heat transfer coefficients in terms of various dimensionless groups of the non-Newtonian slurries studied in this work in laminar flow. The heat transfer coefficients for slurries of half micron and finer kaolin and water are as follows:

1. For a solids content of 12.9 weight percent the heat transfer coefficients ranged from 62.80 to 36.35 for a Reynolds number range of 61.6 to 0.09.
2. For a solids content of 9.6 weight percent the heat transfer coefficients ranged from 74.10 to 50.10 for a Reynolds number range of 156.4 to 1.2.
3. For a solids content of 5.6 weight percent the heat transfer coefficients ranged from 96.90 to 59.25 for a Reynolds number range of 555.5 to 6.0.
4. For a solids content of 3.0 weight percent the heat transfer coefficients ranged from 130.2 to 124.1 for a Reynolds number range of 2020 to 71.7.

The heat transfer coefficients for slurries of two microns and finer kaolin and water are as follows:

1. For a solids content of 23.1 weight percent the heat transfer coefficients ranged from 94.20 to 57.60 for a Reynolds number range of 54.3 to 3.5.
2. For a solids content of 20.4 weight percent the heat transfer coefficients ranged from 99.00 to 55.60 for a Reynolds number range of 81.3 to 5.6.

3. For a solids content of 13.7 weight percent the heat transfer coefficients ranged from 125.2 to 88.10 for a Reynolds number range of 296.1 to 49.9.
4. For a solids content of 10.1 weight percent the heat transfer coefficients ranged from 133.8 to 122.4 for a Reynolds number range of 625.0 to 184.0.

The degree of pseudoplasticity did not significantly change with solids content or particle size for the kaolin slurries studied in this work. However, an increase in solids content increased the viscosity at any given shear rate. Also, at identical solids contents the kaolin of finer particle size gave higher values of viscosity than the coarser material.

NOMENCLATURE

A - Area for heat transfer - ft^2

C - Specific heat - BTU/lb - ^oF

D - Pipe diameter - ft

f - Friction factor - dimensionless

G - Mass velocity - lb/hr - ft^2 of cross section

g - Acceleration due to gravity - 4.17×10^8 ft/hr^2

h - Coefficient of heat transfer between fluid and surface - BTU/hr - ft^2 - ^oF

K - Thermal conducitivity - BTU/hr - ft^2 - $^oF/ft$

L - Length of heat transfer tube - ft.

N - Dimensionless group - i.e. - N_{Re} - Reynolds number

P - Pressure - lb/ft^2

q - Heat transfer rate - BTU/hr

r - Pipe radius - ft

S - Cross section of stream in a tube - ft^2

T - Absolute temperature - ^oR

t - Temperature - ^oF

U - Overall heat transfer coefficient - BTU/hr - ft^2 - ^oF

V - Average velocity - ft/sec

w - Mass rate of flow - lb/hr

x - Percent of dry solids by weight in slurry

Xv - Fraction of solids by volume

Subscripts

b - For bulk

c - For condensate

f - For film

i - For inlet

l - For liquid

m - For log mean temperature

o - For outlet

p - For particle

s - For steam

v - For volume

w - For wall

Greek

Δ - For difference

μ - Viscosity of fluid - lb/hr - ft
centipoises x 2.42

π - 3.1416

ρ - Density of fluid - lb/ft^3

$\dot{\gamma}$ - Shear rate - sec^{-1}

τ - Shear stress - lb/ft^2

BIBLIOGRAPHY

1. Binder, R., and Pollara, P., M.S. Thesis in Chemical Engineering, Newark College of Engineering, Newark, 1954.

2. Bonilla, C. F., Cerui, A., Colven, T. J., and Wang, S. J., Chemical Engineering Progress Symposium Series, No. 5. Vol. 49, 1953, p. 127.

3. Brown, G. G. and Associates, "Unit Operations". John Wiley and Sons, Inc., New York, 1950.

4. Drew, T. B., and Hoopes, J. W. Jr. (Editors), "Advancesin Chemical Engineering", Academic Press Inc., New York, 1956.

5. Eirich, F. R. (Editor), "Rheology", Academic Press Inc., New York, 1960.

6. Green, H., "Industrial Rheology and Rheological Structures", John Wiley and Sons, Inc., New York, 1949.

7. Martinelli, R.C., and Boelter, Publs. Eng., Vol. 5, 1942, p. 23.

8. McAdams, W. H., "Heat Transmission", McGraw-Hill Book Company, Inc., New York, 1954.

9. Metzner, A. B., Vaughn, R. D., Houghton, G. L., A. I. Ch. E. Journal, Vol 3., 1956, p. 92.

10. Miller, A. P., Jr., Ph.D. Thesis in Chemical Engineering, University of Washington, Seattle, 1953.

11. Mooney, M., Journal of Rheology, Vol. 2, 1931, p. 210.

12. Orr, C., Jr., and DallaValle, J. M., Chemical Engineering Progress Symposium Series No. 9, Vol. 50, 1954, p. 29.

13. Ostwald, W., Kollaidschr., Vol. 38, 1926, p. 261.

14. Otto, R. E., and Metzner, A. B. "Agitation of non-Newtonian Fluids", Paper presented at the Seventh Annual Delaware Chemical Symposium, 1955.

15. Perry, J. H. (Editor), "Chemical Engineers Handbook", McGraw-Hill Book Co., Inc., New York, 1950.

16. Pigford, R. L., Chemical Engineering Progress Symposium Series No. 17, Vol. 51, 1955, p. 79.

17. Reiner, M., "Deformation of Flow", Lewis, London, 1949.

18. Roth, W., and Eich, S. R., Journal of Applied Physics, Vol. 24, 1953, p. 940.

19. Salamone, J. J., and Newman, N., Industrial Engineering Chemistry, Vol. 47, 1955, p. 283.

20. Scott-Blair, G. W., "Introduction to Industrial Rheology", J. A. Churchill, London, 1938.

21. Sieder, E. N., and Tate, G. E., Industrial Engineering Chemistry, Vol. 28, 1936, p. 1429.

22. Tareef, B. M., and Baer, V. A., Colloid J. (USSR) 3,771-5 (1937)

23. Taso, G. T., Industrial Engineering Chemistry, Vol. 53, 1961, p. 395.

24. Wilkinson, W. L., "Non-Newtonian Fluids", Pergaman Press Inc., New York, 1960.

25. Winding, C. C., Bittman, P. E., and Kranich, W. L., "Thermal Properties of Synthetic Rubber Latices", Report to Reserve Company, Cornell University, Ithaca, 1944.

APPENDIX

Sample Calculations

Sample Run - Run No. 1 (Refer to Table I for Original Data)

1. Flow Rate (w) = 11 3/8 lbs./30 sec = 1,365 lb/hr

2. Outlet Temperature of Slurry (t_o)
1.90 millivolts thermocouple reading from Figure 4 is 97.6°F.

3. Inlet Temperature of Slurry (t_i)
1.48 millivolts thermocouple reading from Figure 4 is 83.4°F.

4. Temperature Rise of Slurry ($t_o - t_i$) = 97.6 - 83.4 = 14.2°F.

5. Percent Solids (x) Determined by a Cenco Moisture Balance
x = 12.9% Kaolin

6. Specific Heat of Slurry (C_b) = $C_l(1-x) + C_p x$
C_l = Heat Capacity of Water = 1 BTU/lb - °F
C_p = Heat Capacity of Kaolin = .22 BTU/lb - °F
x = Weight Fraction of solid
C_b = 1 (1 - 0.129) + 0.224 (0.129) = 0.900 BTU/lb - °F

7. Slurry Heat (q_b) = (wC_b) (Temp. Rise)
q_b = (1.365) (0.900) (14.2) = 17,440 BTU/hr.

8. Condensate Flow Rate (w_c) = 930 grms/4 min = 17.80 lbs/hr.

9. Enthalpy of Steam (H_s) -
Throttling Steam Calorimeter Data -
Temp. of Steam Before Orifice = 216 °F
Temp. of Steam After Orifice = 180 °F @ 15.70" Hg Vacuum
Barometric Pressure = 29.65" Hg.

Pressure After Orifice = $(29.65 - 15.70)\frac{14.7}{29.92}$ = 6.86 psia
Fluid Enthalpy of Steam at 180°F and 6.86 psia
From Mollier Diagram
H_s = 1138.0 BTU/lb.

10. Enthalpy of Condensate (H_c)
Condensate Temperature = 216°F
H_c from Steam Tables = 214.0 BTU/lb.

11. Heat Given Up by Steam ($H_s - H_c$) = (1138 - 214) = 924 BTU/lb of condensate.

12. Steam Heat (q_s) = (w_c) (ΔH) = (17.70) (924) = 16,360 BTU/hr.

13. Log Mean Temperature Difference Between Slurry Bulk and Pipe Temperature (Δt_m)

#	Pipe Temperature mV	^oF	
2	6.02	236	Bottom of Exchanger
3	6.35	245	
4	6.30	244	
5	6.03	236	
6	6.30	244	
7	6.37	246	Top of Exchanger

Bulk Inlet Temperature = 83.4°F
Bulk Outlet Temperature = 97.6°F

Plot Data As Shown On Following Page (Figure 16)
Area Between Curves = 46.90 in^2
Therefore $\Delta t_m = \frac{46.90\ in^2}{6\ in} \times \frac{20^oF}{in} = 156.5^oF$

14. Experimental Film Coefficient of Heat Transfer (h_f)

$$h_f = \frac{q_s}{A\Delta t_m} = \frac{(16{,}180)}{\left(\frac{1.049\pi}{12}\right)(6)(156.5)} = 62.80\ BTU/hr - ft^2 - {}^oF$$

15. Slurry Density (ρ_b) Found From Figure 3.

X = 12.9% Kaolin
$\rho_b = 67.4\ lb/ft^3$

16. Velocity of Slurry Through Heat Exchanger (V_b)

$$V_b = \frac{(w)(144)}{(\rho_b)\left(\frac{\pi}{4} D^2\right)(3600)}$$

$$V_b = \frac{(1365\ lb/hr)\left(144\ \frac{in^2}{ft^2}\right)}{(67.4\ lb/ft^3)\left(\frac{\pi}{D}\right)(1.049\ in)^2\left(3600\ \frac{sec}{hr}\right)} = 0.937\ ft/sec$$

17. Bulk Viscosity (K_b)

Fann Viscometer Data @ 90.5°F

Speed - RPM	$lbs/100\ ft^2$ (Scale Reading)
3	13.5
6	17.0
100	26.7
200	29.8
300	31.5
600	36.5

FIGURE 10

Determination of Δt_m

Degrees Fahrenheit
vs.
Heat Exchanger Length

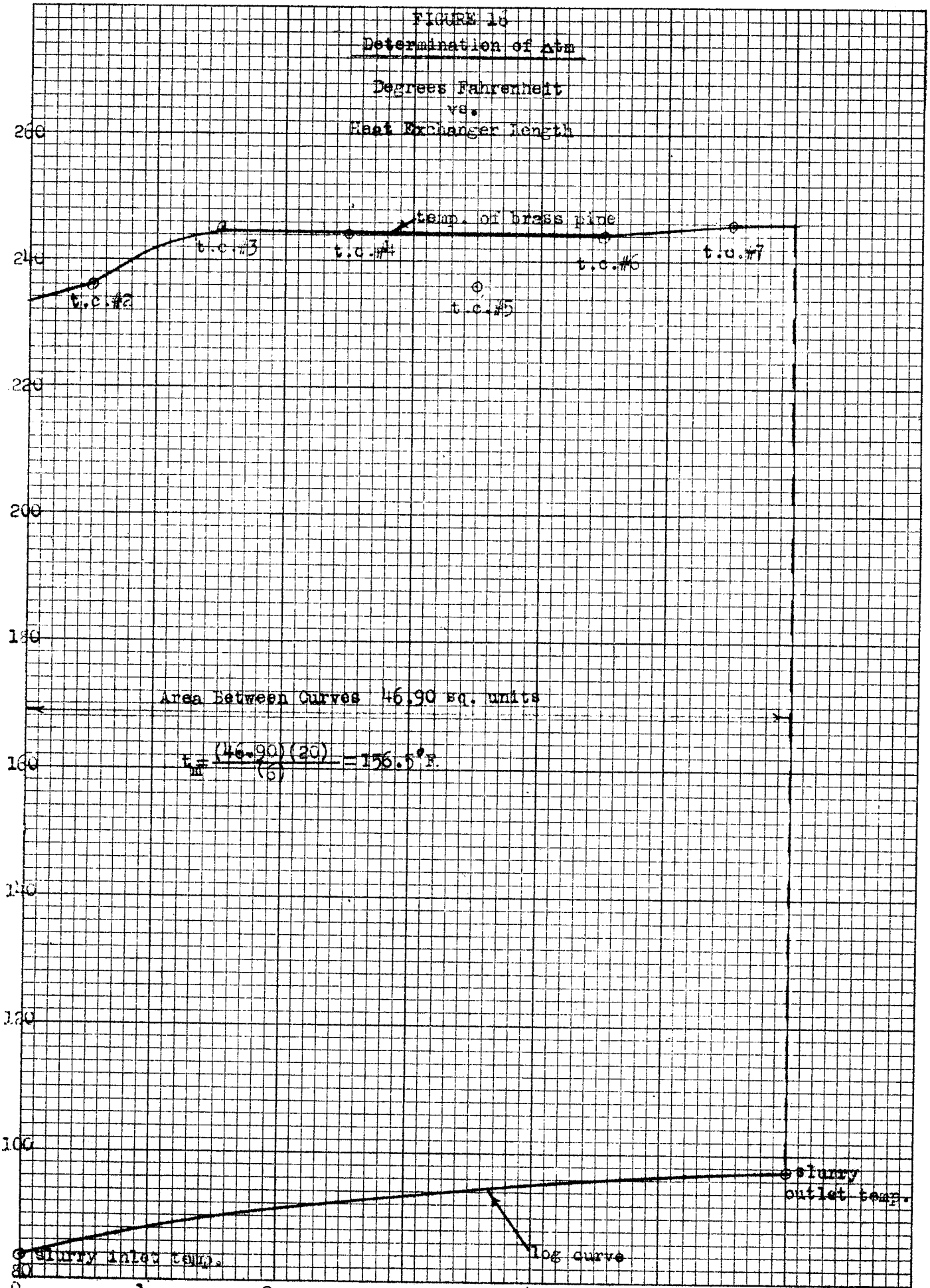

From Above Data Calculate:

Shear rate (γ) = (240) (1.569)

Viscosity (μ) = $\dfrac{\frac{\text{lb}}{100\ \text{ft}^2}\ (100)\ (32.2)}{\frac{1}{\text{sec}}}$

Shear Rate versus Viscosity	
Sec^{-1}	$\frac{\text{lb}}{\text{ft - sec}}$
91.2	0.0125
1.71	0.0215
314	0.0306
157	0.0648
7.12	0.081
4.71	0.922

Above Data plotted on Figure 7

To Find Viscosity of Slurry in Pipe, Calculate Shear Rate (γ)

$$\gamma = \frac{8\ V_b}{D} = \frac{(8)\ (0.937)}{(1.049)\ \frac{1}{12}} = 67.7\ \text{sec}^{-1}$$

Refer to Figure 7 and Find Corresponding Milk Viscosity (μ_b) Having a Shear Rate of 67.7 sec^{-1}.

$$\mu_b = 0.0895\ \frac{\text{lb}}{\text{ft- sec}}$$

18. Reynolds Number (N_{Re}) = $\dfrac{D V_b \rho_b}{\mu_b}$

$$N_{Re} = \frac{1.049}{12}\ \frac{0.937}{0.0895}\ (67.4) = 62.6$$

19. Thermal Conductivity of Slurry (K_b)

$$K_b = K_1 \left[\frac{2K_1 + K_p - 2\lambda_v (K_1 - K_p)}{2K_1 + K_p + \lambda_v (K_1 - K_p)} \right]$$

$\lambda_v = 0.0851$; $K_1 = 0.361$; $K_p = 0.110$

$$K_b = \left[\frac{0.361\ 2(0.361) + 0.110 - 2(0.0851)\ (0.361 - 0.110)}{2\ 0.361) + 0.110 + 0.0851\ (0.361 - 0.110)} \right] = 0.348\ \frac{\frac{\text{Btu}}{\text{hr ft}^2\ \text{°F}}}{\frac{\text{ft}^2}{\text{ft}^2}}$$

20. Prandtl Number (N_{Pr})

$$N_{Pr} = \frac{C_b \mu_b}{K_b} = \frac{(0.900)\ (0.0895)\ (3600)}{(0.348)} = 31.2$$

21. Stanton Number (N_{St})

$$N_{St} = \frac{h_f}{C_b V_b \rho_b} = \frac{(62.3)}{(0.900)\ (0.937)\ (67.4)\ (3600)} = 3.37 \times 10^{-4}$$